Timing, origin and emplacement dynamics of mass flows offshore of SE Montserrat in the last 110 ka: Implications for landslide and tsunami hazards, eruption history, and volcanic island evolution

J. Trofimovs, P. J. Talling, J. K Fisher, M. B Hart, R S J Sparks, S. F L Watt, M. Cassidy, C. W Smart, A. Le Friant, S. G Moreton, et al.

Geochemistry Geophysics Geosystems G3

Article
Volume 14, Number 2
27 February 2013
doi:10.1002/ggge.20052
ISSN: 1525-2027

Published by AGU and the Geochemical Society

Timing, origin and emplacement dynamics of mass flows offshore of SE Montserrat in the last 110 ka: Implications for landslide and tsunami hazards, eruption history, and volcanic island evolution

J. Trofimovs
Queensland University of Technology, Brisbane, Australia (jessica.trofimovs@qut.au)

P. J. Talling
National Oceanography Centre, Southampton, UK

J. K. Fisher and M. B. Hart
School of Earth, Ocean and Environmental Sciences, University of Plymouth, Plymouth, UK

R. S. J. Sparks
Department of Earth Sciences, University of Bristol, Bristol, UK

S. F. L. Watt and M. Cassidy
National Oceanography Centre, Southampton, University of Southampton, Southampton, UK

C. W. Smart
School of Geography, Earth and Environmental Sciences, Plymouth University, Plymouth, UK

A. Le Friant
Institut de Physique du Globe de Paris & CNRS, Paris, Cedex 05, France

S. G. Moreton
NERC Radiocarbon Facility (Environment), Scottish Enterprise Technology Park, East Kilbride, UK

M. J. Leng
NERC Isotope Geosciences Laboratory, British Geological Survey, Keyworth, Nottingham, UK

[1] Mass flows on volcanic islands generated by volcanic lava dome collapse and by larger-volume flank collapse can be highly dangerous locally and may generate tsunamis that threaten a wider area. It is therefore important to understand their frequency, emplacement dynamics, and relationship to volcanic eruption cycles. The best record of mass flow on volcanic islands may be found offshore, where most material is deposited and where intervening hemipelagic sediment aids dating. Here we analyze what is arguably the most comprehensive sediment core data set collected offshore from a volcanic island. The cores are located southeast of Montserrat, on which the Soufriere Hills volcano has been erupting since 1995. The cores provide a record of mass flow events during the last 110 thousand years. Older mass flow deposits differ significantly from those generated by the repeated lava dome collapses observed since 1995. The oldest mass flow deposit originated through collapse of the basaltic South Soufriere Hills at 103–110 ka, some 20–30 ka after eruptions formed this volcanic center. A ~1.8 km^3 blocky debris avalanche deposit that extends from a chute in the island shelf records a particularly deep-seated failure. It likely formed from a collapse of almost equal amounts of volcanic edifice and coeval carbonate shelf, emplacing a mixed bioclastic-andesitic

turbidite in a complex series of stages. This study illustrates how volcanic island growth and collapse involved extensive, large-volume submarine mass flows with highly variable composition. Runout turbidites indicate that mass flows are emplaced either in multiple stages or as single events.

Components: 12,500 words, 7 figures, 1 table.

Keywords: Montserrat; mass flow; submarine; stratigraphy.

Index Terms: 3070 Volcanoclastic deposits:

Received 22 October 2012; **Revised** 17 December 2012; **Accepted** 18 December 2012; **Published** XX Month 2013.

Trofimovs, J., P. J. Talling, J. K. Fisher, R. S. J. Sparks, S. F. L. Watt, M. B. Hart, C. W. Smart, A. Le Friant, M. Cassidy, S. G. Moreton, and M. J. Leng (2013), Timing, origin and emplacement dynamics of mass flows offshore of SE Montserrat in the last 110 ka: Implications for landslide and tsunami hazards, eruption history, and volcanic island evolution, *Geochem. Geophys. Geosyst.*, *14*, 385–406, doi:10.1002/ggge.20052.

1. Introduction

[2] Mass flows from volcanic islands can pose a serious hazard to property and life. The collapse of lava domes can generate destructive pyroclastic flows, which in turn may produce tsunamis as they enter the sea. For instance, a series of dome collapse pyroclastic flows have devastated parts of the island of Montserrat in the Lesser Antilles during its ongoing eruption (1995 to present). The largest dome collapse (0.2 km^3) produced a tsunami that locally ran up to 15 m around Montserrat's coastline [*Herd et al*., 2005]. This tsunami reached neighboring islands where it had an amplitude of a few tens of centimeters [*Herd et al*., 2005]. Deeper-seated collapse of volcanic edifices can generate much larger-volume mass flows that include some of the largest seen on Earth [*Masson et al*., 2006 and references therein]. These flank collapses can potentially form larger-magnitude tsunamis whose impact is felt over wider areas [*Masson et al*., 2006]. The magnitude of such tsunamis is uncertain and controversial, as we are yet to monitor such a collapse in detail, with tsunami magnitude highly dependent on the manner in which the collapse progresses (as one or multiple stages) including its volume and acceleration. Mapping of the sea floor around Montserrat and neighboring volcanic islands has identified over 40 major landslides, with 15 events in the last 12 ka [*Boudon et al*., 2007]. It is important to better understand the frequency, temporal clustering and relation to eruption cycles, and emplacement dynamics of these different types of mass flow from volcanic islands.

[3] The record of mass flows from volcanic islands is often difficult to reconstruct from deposits found on land, as these deposits may be eroded or bypass offshore. For instance, at least 65% of the material erupted since 1995 by the Soufriere Hills volcano on Montserrat has ended up in the ocean [*Le Friant et al*., 2010]. Moreover, deposits on land may be buried and inaccessible. The offshore marine record of mass flows is more complete and more easily deciphered. Marine mass flow deposits also typically have intercalated intervals of carbonate-rich hemipelagic sediment that allows them to be dated.

[4] Here we analyze the record of mass flows offshore of Montserrat using an unusually comprehensive set of marine cores that extend for up to 5 m below the sea floor. Montserrat is an excellent location at which to study the frequency and emplacement dynamics of mass flows from volcanic islands. The ongoing eruption of the Soufriere Hills volcano has been studied in almost unprecedented detail, including the subaerial dynamics of andesite lava dome collapses and associated pyroclastic flows that have reached the ocean [e.g., *Druitt and Kokelaar*, 2002; *Cole et al*., 2002; *Herd et al*., 2005; *Voight et al*., 2006]. The offshore continuation of 1995 to recent pyroclastic flows has been studied through repeated bathymetric mapping and sediment coring [e.g., *Deplus et al*., 2001; *Le Friant et al*., 2004; 2008; 2010; *Trofimovs et al*., 2006; 2008; 2012]. This is the only location where deposits from the submarine continuations of dome collapse pyroclastic flows have been studied in such detail. The data collected from the current eruption aids the recognition and interpretation of submarine mass flows related to older dome collapses.

[5] The eruptive history of the Soufrière Hills-South Soufrière Hills volcanic complex during the last 170 ka has also been relatively well studied [*Rea*, 1974; *Roobol and Smith*, 1998; *Harford et al*., 2002; *Smith et al*., 2007]. For example,

Harford et al. [2002] produced a detailed geochronological record for the subaerial lava domes and pyroclastic deposits on Montserrat using Ar^{40}/Ar^{39} dating techniques. This work established that the currently active Soufrière Hills volcano is at least 174 ka old and identified a distinctive period of basaltic volcanism associated with the South Soufrière Hills volcanic complex at 125–131 ka. *Le Friant et al*. [2008] studied the micropaleontology, oxygen isotope stratigraphy, and tephrochronology of a marine sediment core recovered ~55 km SW of Montserrat (16°27.699′N, 62°38.077′W). The core is 575 cm long and dates back to circa 250 ka. This core records 15 eruptive events, including four previously unknown from the subaerial record, helping us to compare the timing of mass flow deposits with the timing of major eruptions.

[6] This paper is based on the results of a research voyage of the RRS *James Clark Ross* (cruise JR123; 9–18 May 2005) that collected 56 vibrocores from the seafloor off the east and southeast coast of Montserrat (Figure 1). Previous publications have described the character of the 1995 to recent eruption products found in these cores [*Trofimovs et al*., 2006; 2008] and the character of the most powerful mass flow event seen in the cores, a distinctive mixed volcanic-bioclastic mass flow deposit emplaced around 14,000 years ago [*Trofimovs et al*., 2010]. This contribution presents the full stratigraphy of mass flow deposits seen in these cores and includes a more detailed chronological framework, incorporating additional radiocarbon dates. This includes major mass flow events that were not analyzed previously. Additional information is used to revise the most likely origin and significance of the mixed volcanic-bioclastic deposit, which we refer to as the ~12–14 ka event [*Trofimovs et al*., 2010]. This new contribution includes a discussion of the full record of events rather than focusing on a specific mass flow deposit, allowing their timing and character to be compared to the terrestrial record of eruptions, and the distal marine record of pyroclastic eruption fallout [*Le Friant et al*., 2008].

1.1. Aims

[7] The overall objective of this contribution is to understand the timing, composition, and character of submarine mass flow events offshore of SE Montserrat during the last 110 ka. The first aim is to determine the source and most likely trigger for each mass flow event, such as dome collapse, deeper-seated volcanic edifice collapse, or collapse of carbonate shelf material around the volcanic edifice. The second aim is to understand how each mass flow was emplaced in single or multiple stages. The third aim is to document the frequency of these different types of mass flow event. The fourth aim is to analyze how mass flows might be related to volcanic eruption cycles. In particular, is there evidence that the mass flows were associated with major volcanic eruptions? This contribution helps to understand the growth and collapse of a particularly well-studied volcanic island over a 110 ka period. It also provides general insights into the frequency, timing, and emplacement dynamics of mass flows that can aid hazard assessment elsewhere.

2. Geological Setting

[8] The volcanic island of Montserrat is situated at the northern end of the Lesser Antilles island arc (Figure 1a), which results from subduction of the North American plate beneath the Caribbean plate with a convergence rate of 2–4 cm/year [*Bouysse et al*., 1990; *Zellmer et al*., 2003; *Grindlay et al*., 2005]. North of Dominica, the arc bifurcates into two island chains, the Outer (eastern) Limestone Caribbees and the Inner (western) Volcanic Caribbees [*Nagle et al*., 1976; *Briden et al*., 1979; *Bouysse et al*., 1990]. South of the bifurcation, the arc consists of a single string of islands, in which the two chains are superimposed. Arc volcanism initiated at circa 40 Ma and continues today with magma productivity within the arc being relatively low (<3–$5\ km^3\ Ma^{-1}\ km^{-1}$ of arc; *Wadge* [1984]). Volcanism is focused within the Inner Volcanic Caribbees, which contains 12 active volcanoes, including Montserrat.

[9] The island of Montserrat comprises three volcanic massifs (Figure 1b). Each massif comprises a central core of andesite lava dome rock surrounded by talus aprons and pyroclastic deposits predominantly resulting from dome failure. The northernmost, Silver Hills massif (circa 2600–1200 ka; *Harford et al*. [2002]) has been exposed to long-term terrestrial and coastal erosion, producing a 5 km-wide, shallow (60–100 m depth) submarine shelf around the northern part of the island [*Le Friant et al*., 2004]. The Centre Hills massif (circa 950–550 ka; *Harford et al*. [2002]) has been subjected to less erosion than the Silver Hills and exhibits high-relief terrane with a deeply gullied surface. The submarine shelf adjacent to the Centre Hills is 1–3 km wide. The youngest Soufrière Hills-South Soufrière Hills complex (circa 170 ka to present; *Harford et al*. [2002]) has yet to undergo significant erosion. Recent dome collapse pyroclastic density currents have increased the landmass in

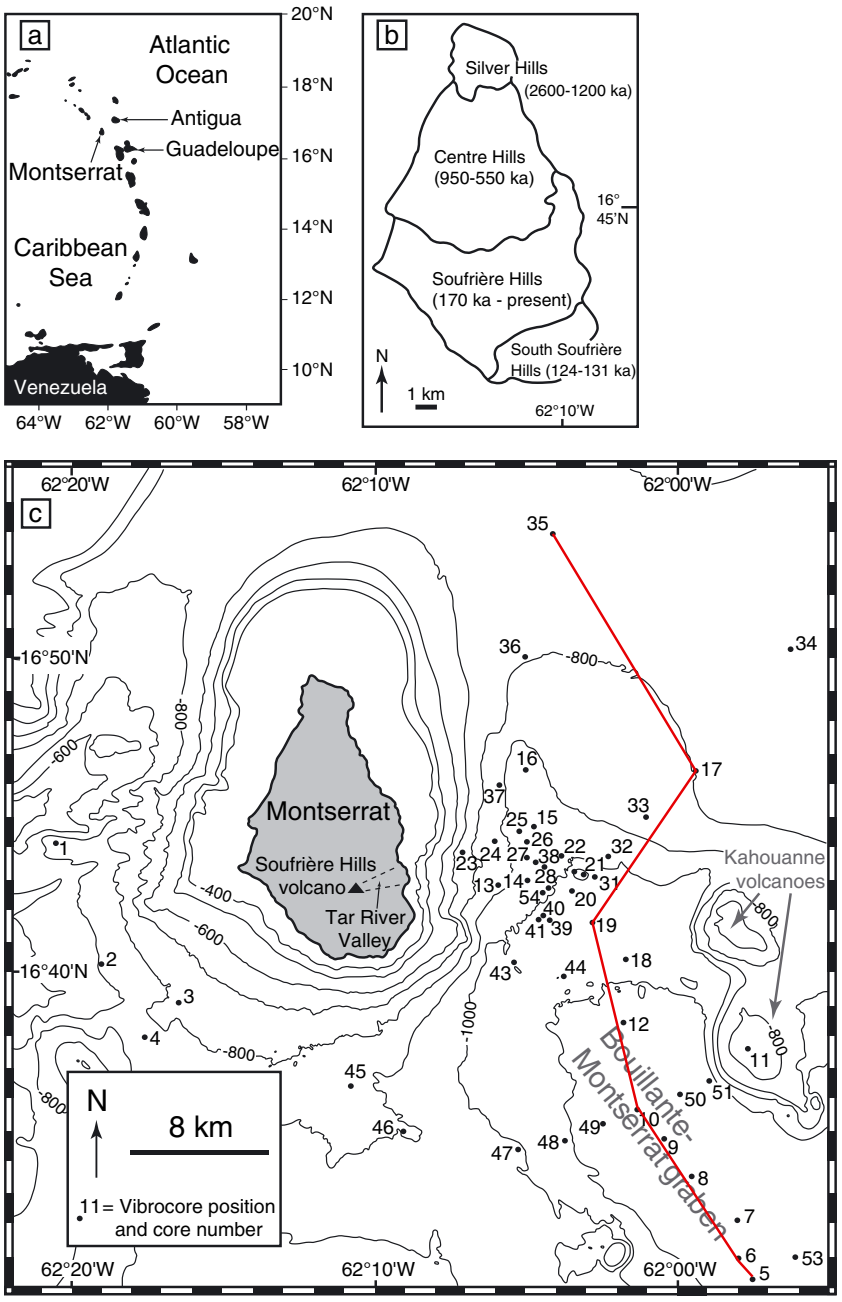

Figure 1. (a) Map of the Lesser Antilles island arc showing the location of Montserrat. (b) Map of Montserrat depicting the three volcanic complexes (Silver Hills, Centre Hills, and the combined Soufrière Hills-South Soufrière Hills volcanic massifs), with dates. (c) Seafloor bathymetry around Montserrat with the number and location of the marine sediment cores. Red line denotes profile in Figure 2.

this region, and consequently only a narrow, approximately 0.5 km-wide submarine shelf surrounds the southern section of Montserrat [*Le Friant et al.*, 2004].

[10] The morphology of the Soufrière Hills volcano has been shaped by flank collapses. Much of the recent (1995 to present) lava dome growth and collapse activity has been focused within a large east-facing horseshoe-shaped amphitheater called English's Crater. This structure has an evacuated volume of approximately 0.5 km^3. *Roobol and Smith* [1998] propose an age of 3950 ± 70 years B.P. for the flank failure that created English's crater. However, *Boudon et al.* [2007] identify a subsequent collapse that partially in-filled English's Crater at 1990 ± 30 year B.P., which may have contributed to the collapse scar morphology. The

most recent flank collapse occurred on the 26 December 1997 when a 40–50 $\times 10^6$ m^3 section of the volcano failed because of weakness due to hydrothermal alteration [*Voight et al.*, 2002; *Young et al.*, 2002]. The resulting debris avalanche traveled down the White River Valley towards the south of the island, stopping 20 m from the shore.

[11] The current eruption of the Soufrière Hills volcano (1995 to present) has predominantly involved porphyritic andesite lava dome growth, collapse, and repose phases, with subordinate Vulcanian activity. The volcanic deposits produced during the early part of the eruption (1996–1997) were distributed radially around the volcano [*Cole et al.*, 2002]. Since 1998, activity has been dominantly confined within English's Crater as dome growth and seven major pyroclastic dome collapses have transported material down the Tar River Valley (Figure 1c) and into the ocean off the east coast of Montserrat [*Herd et al.*, 2005; *Trofimovs et al.*, 2006], amalgamating to form an elongate fan. This material has also extended the original coastline at the mouth of the valley by approximately 600 m. The majority of the deposits, however, have been transported off the narrow shelf into deeper ocean (>500 m depth; *Trofimovs et al.* [2006]). The submarine volcano flanks in this region have a slope of around 35°, shallowing at ~500 m water depth to ~9.5°, and then after a second break in slope at ~750 m water depth to <2.5° [*Trofimovs et al.*, 2008]. The seafloor slopes gently towards the southeast within the fault-bound Bouillante-Montserrat Graben (Figure 1c). The graben acts as a submarine sediment depocenter for pyroclastic material shed from the southern and eastern flanks of the Soufrière Hills volcano.

[12] Detailed 2-D and 3-D seismic data have documented a series of major landslide deposits within the Bouillante-Montserrat graben [*Deplus et al.*, 2001; *Le Friant et al.*, 2009; *Lebas et al.*, 2011; *Watt et al.*, 2012a; 2012b]. The youngest deposit (deposit 1) is characterized by a chaotic seismic character and abundant randomly distributed blocks that protrude from the sea floor and are up to 200 m across. The presence of these blocks suggests emplacement primarily as a granular debris avalanche [*Masson et al.*, 2006]. Deposit 1 has a near semicircular outline that extends ~12 km from the coast, where it terminates on gradients of ~1° [*Le Friant et al.*, 2004; *Lebas et al.*, 2011; *Watt et al.*, 2012a]. It has a volume of ~1.8 km^3 [*Lebas et al.*, 2011] and originates from the northern part of a chute cut into the shelf offshore from the Tar River Valley. It has been proposed that deposit 1 resulted from the formation of English's Crater. Even allowing for expansion of the failed material in English's Crater (0.5 km^3), the debris avalanche must have incorporated sediment from the submerged volcano or shelf to achieve its final volume. The volume of eroded material represented by the chute is about 0.5 to 1.1 km^3 [*Watt et al.*, 2012a]. Seismic profiles show that the sediment drape over deposit 1 cannot be resolved and is therefore <5 m, consistent with an emplacement age during the last few tens of thousands of years [*Watt et al.*, 2012a]. By correlating with the deposit infilling part of English's crater, *Boudon et al.* [2007] proposed an age of ~2 ka for deposit 1.

[13] Seismic data also document the presence of much larger older-landslide deposits in the Bouillante-Montserrat graben [*Lebas et al.*, 2011; *Watt et al.*, 2012b]. However, these are buried by at least 5–10 m of sediment and would not be intersected by the sediment cores used in this study. Two blocky avalanche deposits (deposits 3 and 5) occur to the south of Montserrat which are buried by only a few meters of sediment [*Lebas et al.*, 2011]. These debris avalanche events could potentially have triggered mass flows that reached the study area.

3. Methods

[14] The focus of the 9–18 May 2005 research cruise (JR123) was to sample the July 2003 dome collapse, which was the largest historic dome collapse globally, involving 210 $\times 10^6$ m^3 of dome material [*Herd et al.*, 2005]. An initial high-resolution EM 120 swath bathymetric survey of the study area, together with TOPAS sub-bottom profile surveys, identified sites with a shallow gradient and absence of rough topography suitable for coring [*Trofimovs et al.*, 2006].

[15] A Vibrocore system developed by the British Geological Survey was used to recover up to 5 m of unconsolidated volcanic sediment in less than 2000 m of water. Fifty-two cores were recovered, predominantly from the east and southeast of Montserrat within the Bouillante-Montserrat graben (Figure 1). The cores were halved down their length onboard the ship for stratigraphic logging and then placed in cold storage (4–5°C). On land, they were subsampled for analysis by taking quarter-core slices 1 cm in length. On removal of the sediment, the void was packed with polystyrene to stop the remaining core collapsing.

[16] The coarse-grained nature of the sampled sediment necessitated the use of nested sieve sets for grain size analysis. Samples were dried at 90°C for 48 h before being gently disaggregated with a rubber pestle and mortar and dry sieved. Phi (ϕ) sieve intervals were measured between 64 mm and 4 mm (-6ϕ to -2ϕ), and half phi intervals were measured between 4 mm and 0.045 mm (-2ϕ to 4.5ϕ). Component abundance was obtained by bulk point counting a minimum of 500 grains from each studied sample.

[17] Selected cores were subsampled at 5 cm intervals through their entire length for oxygen isotope and micropaleontological studies. The sediment was soaked in deionized water and washed over a 0.063 mm stainless steel sieve. The >0.063 mm size fraction was collected, filtered, and dried and processed through a 0.15 mm sieve. The >0.15 mm size fraction was used for microfaunal counts of foraminifera and pteropods.

[18] The <0.063 mm size fraction was collected, filtered, and dried in a cool (35–40°C) oven before being homogenized with an agate mortar and pestle and sent for oxygen isotope analysis at the Natural Environment Research Council Isotope Geosciences Laboratory, British Geological Survey, Keyworth. The carbonate sample was reacted with anhydrous phosphoric acid in vacuo overnight at a constant 25°C. The carbon dioxide liberated was separated from water vapor under vacuum and collected for analysis by a VG Optima mass spectrometer. Analytical reproducibility for these samples was better than 0.1‰ for $\delta^{13}C$ and $\delta^{18}O$. Isotope values ($\delta^{13}C$, $\delta^{18}O$) are reported as per mil (‰) deviations of the isotopic ratios ($^{13}C/^{12}C$, $^{18}O/^{16}O$) calculated to the Vienna Pee Dee Belemnite (VPDB) scale using a within-run laboratory standard calibrated against National Bureau of Standards isotope standards.

[19] Samples were also collected for accelerator mass spectrometry (AMS) ^{14}C dating at the Scottish Universities Environmental Research Centre (SUERC) AMS Laboratory and Beta Analytical laboratories. These samples were taken from hemipelagic sediment deposited directly above and below the deposits targeted for dating. Hemipelagic sediment was distinguished from fine-grained turbidite mud by the presence of 60–70 vol % dominantly pristine (unbroken or abraded) foraminifera in a structureless clay-rich substrate. Areas exhibiting bioturbation were avoided as these can produce erroneous dates due to vertical mixing of foraminifera within the core. Samples were processed using deionized water to disaggregate the sediment, before being washed over a 0.063 mm sieve, dried, and dry sieved over a 0.15 mm sieve. The >0.15 mm fraction was used to handpick specimens for dating: 12–14 mg of monospecific sample material (*Globigerinoides ruber* tests) were picked with the exclusion of specimens showing any visual signs of reworking or diagenesis. Known weights of the sample were hydrolyzed to CO_2 using 85% orthophosphoric acid. A subsample of the CO_2 was analyzed for $^{13}C/^{12}C$ ratios using a dual inlet stable isotope mass spectrometer (VG OPTIMA). The $^{13}C/^{12}C$ ratios were used to normalize ^{14}C values to $-25‰$ $\delta^{13}C_{VPDB}$. A subsample of the CO_2 was converted to graphite by iron/zinc reduction [*Slota et al.*, 1987], and the activity of the ^{14}C was determined using either a NEC 5 MV AMS (*Xu et al.*, 2004) or a NEC 250 kV single-stage AMS [*Freeman et al.*, 2008]. The dating results are reported as conventional radiocarbon years before present (relative to AD 1950) and % modern ^{14}C, both expressed at the $\pm 2\sigma$ level for overall analytical confidence. The dates were calibrated against the Marine04 dataset using CALIB 5.0.2 Radiocarbon Calibration software. The Marine04 dataset calibrates ages between 0 and 26 ka; therefore, dates older than this are presented in uncalibrated radiocarbon years.

4. Results

4.1. Radiocarbon (AMS) Dating and Stable Isotope Analysis

[20] A chronological framework for the stratigraphic sequence east of Montserrat was established using oxygen isotope stratigraphy and AMS ^{14}C dating. The hemipelagic sediment between the volcanic and bioclastic event horizons in cores 5-V, 6-V, 10-V, 17-V, 19-V, and 35-V (Figure 2) provided reliable $\delta^{18}O$ stratigraphies. Isotope data from within mass flow deposits was omitted from the stratigraphic analysis as the isotopic signature from within these units is unreliable due to erosion and incorporation of older sediment, as well as vertical mixing within the flow prior to deposition.

[21] Core 6-V, located southeast of Montserrat within the Bouillante-Montserrat graben (Figure 1), contains the longest hemipelagic sediment record. Stable isotope stage boundaries can be identified down to Marine Isotopic Stage 5 (MIS 5.4), indicating that this core preserves a sediment record back to circa 110 ka [*Martinson et al.*, 1987]. Core 5-V also preserves a long history of sedimentation down to MIS 5.31, which corresponds to circa 96 ka [*Martinson et al.*, 1987]. Good age and event

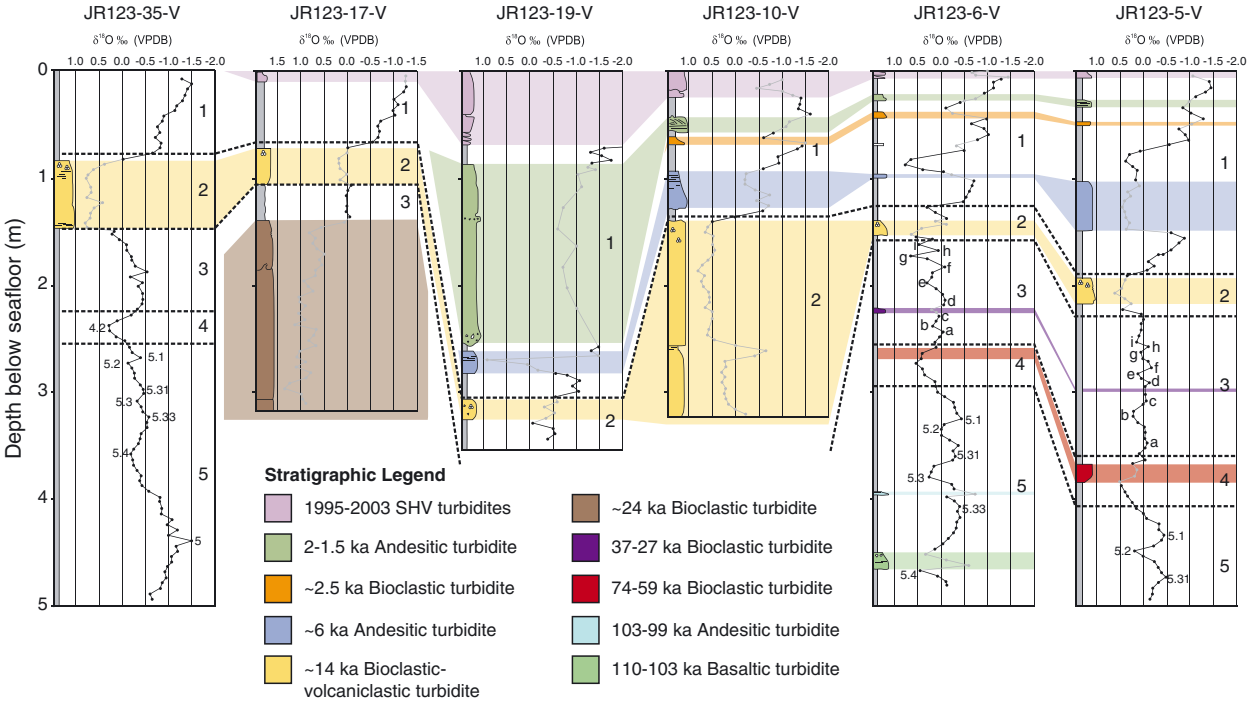

Figure 2. Oxygen isotope ($\delta^{18}O$) stratigraphy measured for cores 35-V, 17-V, 19-V, 10-V, 6-V, and 5-V (see Figure 1 for locations). Each core is presented with marine isotope stages (1 to 5) labeled on the right-hand side of each panel. Samples taken from within the flow or fallout units are shaded gray. Analysis of the stable isotope record in the text avoids this data.

horizon correlation is observed between all of the sediment cores (Figure 2).

[22] The stable isotope profiles are complemented with AMS radiocarbon dating from hemipelagic sediment samples above and below the event horizons (Table 1; Figures 3–5, and 6). A date from the top of the targeted deposit provides the closest estimate for the timing of the end of deposition as it represents the material sedimented directly after the event. Dates at the base of the targeted deposits, particularly mass flow event horizons, provide an estimate of how much material (if any) may have been eroded by the passage of the flow. Using both the oxygen isotope profiles and the ^{14}C AMS dates, an accurate chronostratigraphic record was developed. The accurately dated stratigraphy for the deposits located east and southeast of Montserrat (Figures 2–5, and 6) are described in ascending order below.

5. Submarine Mass Flow Deposits Offshore of SE Montserrat

5.1. Volcanic-sourced Basalt-rich Deposit (between 110 and 103 ka)

[23] The oldest depositional unit recovered from the Bouillante-Montserrat graben comprises angular coarse sand-sized particles of basaltic scoria (~45%), broken olivine, and clinopyroxene crystals (~30%) and subordinate andesitic lava fragments (~25%) (depth interval 4.50–4.63 m; core 6-V). The depositional unit is normally graded, exhibiting a massive base overlain by crude planar stratification, defined by alternation between basalt- and andesite-rich horizons. The unit has a fine-grained top containing ripped up hemipelagic mud/silt clasts. Oxygen isotope profiles have dated this deposit at between circa 110 ka and circa 103 ka (between MIS 5.4 and MIS 5.33; *Martinson et al*. [1987]).

5.2. Volcanic-sourced Andesitic Deposit (between 103 and 99 ka)

[24] A 4 cm thick andesitic deposit with a massive scoured base and top comprising planar laminae is preserved in core 6-V (depth interval 3.92–3.96 cm) between MIS 5.33 and MIS 5.3. This provides an age range of between 103–99 ka [*Martinson et al*., 1987]. The andesitic deposit predominantly comprises plagioclase and hornblende phyric andesite lava clasts, broken plagioclase, hornblende, pyroxene and magnetite crystals and 1–2% bioclastic clasts of broken shell, coral, and carbonate sand particles.

Table 1. Radiocarbon Data for the Submarine Stratigraphy SE of Montserrat

Publication Code	Core Number	Depth (cm) below Sea Floor	Radiocarbon Age (Years B.P. ± 1σ)	$\delta^{13}C_{VPDB}$‰ ± 0.1	Calibrated Ages 1σ	Calibrated Ages 2σ
SUERC-18966	JR123-5-V	39.5	3371 ± 37	0.9	2794 ± 94	2793 ± 237
SUERC-18385	JR123-5-V	152.5	9366 ± 36	0.8	9678 ± 133	9749 ± 261
SUERC-18386	JR123-5-V	157.5	9859 ± 40	1.0	10345 ± 99	10359 ± 175
SUERC-18387	JR123-5-V	217.5	34475 ± 361	0.7	*	*
SUERC-12986	JR123-6-V	17.5	2051 ± 35	0.9	1243 ± 87	1231 ± 189
SUERC-12987	JR123-6-V	29.0	2912 ± 35	0.8	2219 ± 102	2212 ± 228
SUERC-12988	JR123-6-V	46.5	3762 ± 35	1.1	3267 ± 108	3243 ± 227
SUERC-18968	JR123-6-V	60.5	4858 ± 37	1.0	4691 ± 113	4647 ± 221
SUERC-18971	JR123-6-V	70.5	6152 ± 37	0.9	6202 ± 98	6187 ± 201
SUERC-18389	JR123-6-V	98.5	8888 ± 39	1.0	9151 ± 119	9185 ± 217
SUERC-18392	JR123-6-V	138.5	11830 ± 41	0.9	12989 ± 76	13000 ± 140
SUERC-18393	JR123-6-V	158.5	39354 ± 659	0.9	*	*
SUERC-23049	JR123-7-V	119.0	8407 ± 38	1.0	8496 ± 98	8501 ± 173
SUERC-23050	JR123-7-V	144.0	9863 ± 38	1.0	10354 ± 101	10361 ± 173
SUERC-23052	JR123-9-V	36.0	2145 ± 35	1.1	1336 ± 88	1345 ± 181
SUERC-23053	JR123-9-V	60.0	3151 ± 37	0.9	2546 ± 123	2524 ± 201
SUERC-23054	JR123-9-V	75.0	5468 ± 35	1.4	5478 ± 91	5457 ± 177
SUERC-18394	JR123-10-V	39.5	2266 ± 37	0.5	1445 ± 97	1474 ± 191
SUERC-18964	JR123-10-V	69.0	3767 ± 37	0.9	3271 ± 108	3250 ± 230
SUERC-18373	JR123-10-V	89.5	5938 ± 37	1.2	5989 ± 107	5966 ± 215
SUERC-18965	JR123-10-V	129.5	7263 ± 38	1.3	7408 ± 83	7407 ± 156
SUERC-18374	JR123-10-V	134.5	9598 ± 39	1.0	10048 ± 124	9987 ± 251
SUERC-18974	JR123-12-V	38.0	2893 ± 37	0.9	2205 ± 104	2185 ± 225
SUERC-18975	JR123-12-V	84.0	3695 ± 37	1.0	3193 ± 118	3165 ± 227
SUERC-18378	JR123-17-V	72.0	12377 ± 41	0.4	13462 ± 111	13479 ± 198
SUERC-18379	JR123-17-V	137.0	20792 ± 78	1.1	23987 ± 160	24005 ± 327
SUERC-18972	JR123-18-V	35.0	2255 ± 37	0.4	1435 ± 95	1464 ± 190
SUERC-18973	JR123-18-V	146.0	6595 ± 37	1.0	6677 ± 110	6682 ± 218
SUERC-12989	JR123-19-V	85.5	2142 ± 35	0.7	1333 ± 88	1343 ± 182
SUERC-12990	JR123-19-V	262.5	4469 ± 35	1.2	4166 ± 131	4161 ± 242
SUERC-12993	JR123-19-V	285.5	9236 ± 35	1.0	9546 ± 96	9595 ± 222
SUERC-18369	JR123-19-V	310.0	11361 ± 40	0.9	12689 ± 103	12567 ± 258
SUERC-18383	JR123-35-V	60.0	9762 ± 38	0.9	10265 ± 100	10280 ± 214
SUERC-18377	JR123-35-V	148.5	38447 ± 588	1.1	*	*
SUERC-23059	JR123-48-V	324.0	>45326	1.1	*	*
SUERC-23051	JR123-50-V	176.0	9579 ± 38	1.1	10031 ± 127	9973 ± 250
SUERC-23048	JR123-51-V	199.0	9046 ± 38	1.1	9360 ± 97	9318 ± 198
SUERC-12994	JR123-54-V	235.0	6802 ± 35	0.9	6932 ± 118	6936 ± 217
SUERC-12995	JR123-54-V	242.0	6330 ± 35	0.9	6379 ± 91	6405 ± 191
SUERC-23055	JR123-54-V	273.0	8794 ± 37	1.0	9072 ± 126	9027 ± 269
333973	JR123-54-V	280. 0	8700 ± 40	0.1	–	9880 ± 210
333974	JR123-54-V	284.0	8600 ± 40	1.7	–	9660 ± 140
333975	JR123-54-V	294.5	9350 ± 40	4.4	–	10540 ± 60
333976	JR123-54-V	303.0	10830 ± 50	1.1	–	12730 ± 110

*Too old for Marine04 calibration.

5.3. Bioclastic Deposits (74–59 ka, 37–27 ka and ~24 ka)

[25] Two deposits, represented as single depositional units, containing dominantly bioclastic material (99%) are identified at 74–59 ka (core 5-V, depth interval 3.62–3.88 m, within MIS 4) and 37–27 ka (core 6-V, depth interval 2.21–2.26 m, between MIS 3c and MIS 3b). Both deposits are normally graded and consist of fine sand-sized particles of broken shell and foraminifera together with carbonate mud. A subordinate proportion (~1%) of andesitic lava fragments has been incorporated into the deposits; these are commonly concentrated along the scoured bases of the deposits.

[26] A thicker bioclastic deposit, AMS radiocarbon dated at circa 24 ka (from overlying hemipelagic sediment, Table 1), is preserved within core 17-V (Figure 4) and is represented by a minimum

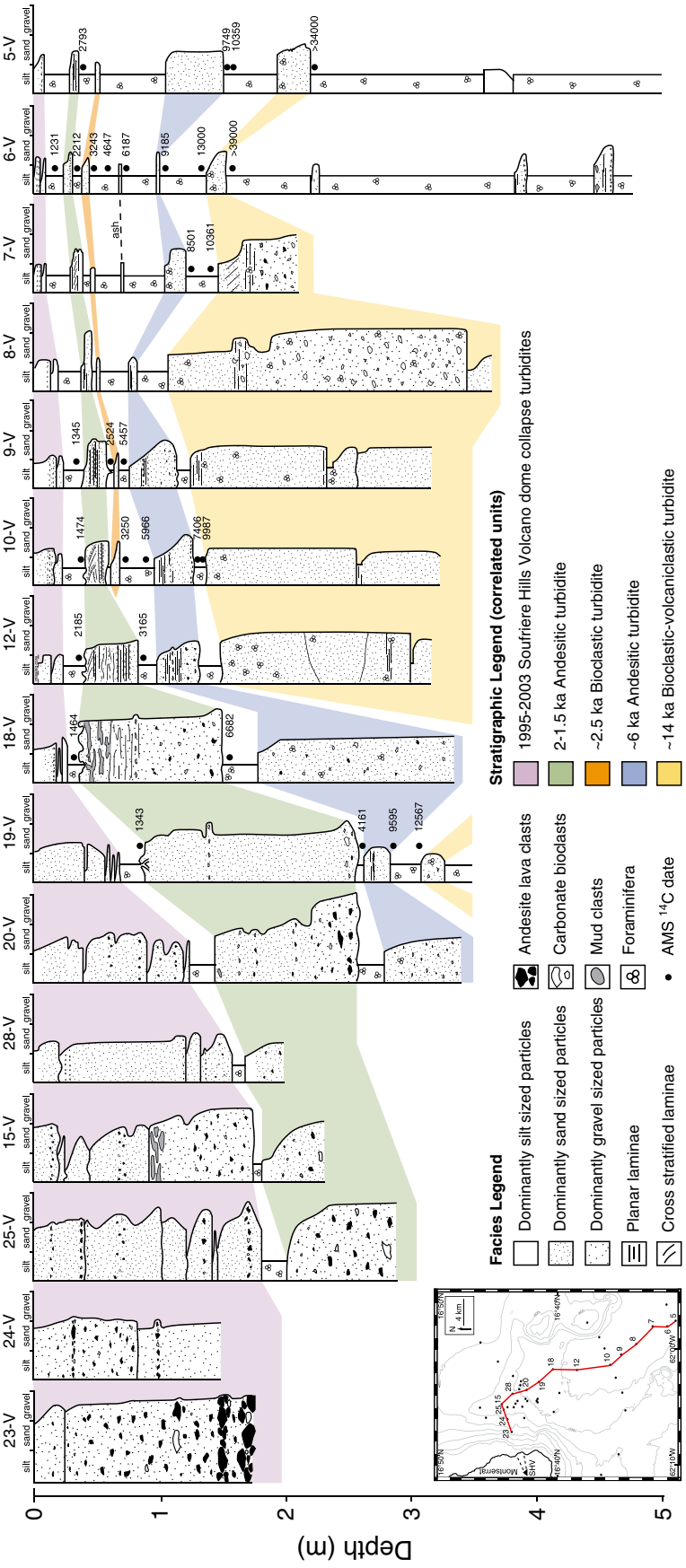

Figure 3. Correlated stratigraphic logs for cores recovered along the central axis of the Bouillante-Montserrat graben. Radiocarbon dates are provided in "years before present" with 2σ standard deviation; full details are in Table 1. Inset map shows the core numbers and locations.

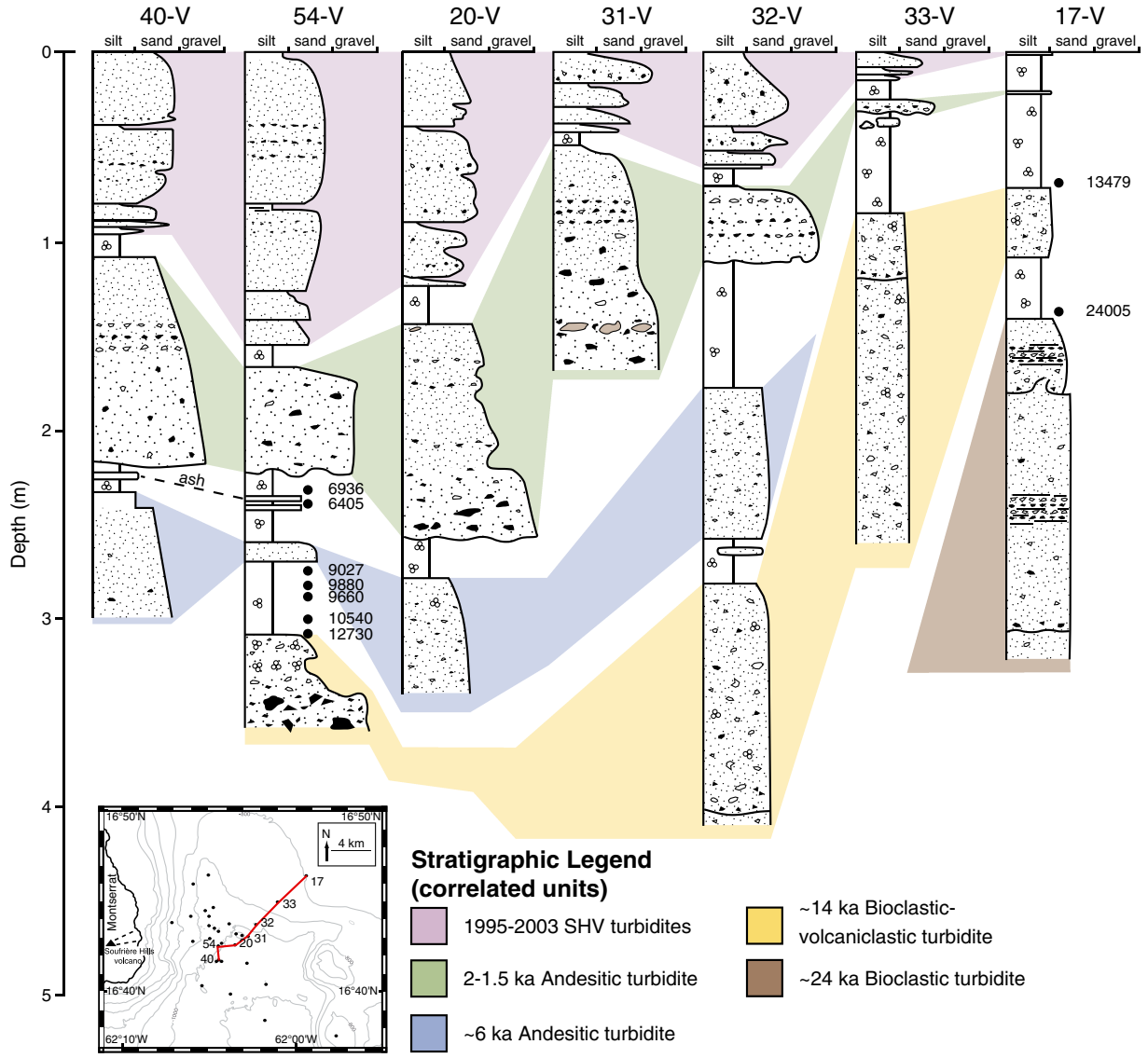

Figure 4. Correlated stratigraphic logs showing a transect through the northern Bouillante-Montserrat graben, perpendicular to the longitudinal graben axis. Radiocarbon dates are provided in "years before present" with 2σ standard deviation; full details are in Table 1. Inset map shows the core numbers and locations.

thickness of 1.40 m (the base was not intersected). The deposit is represented by three normally graded depositional subunits. Each subunit comprises dominantly bioclastic material (94–98%) with varying proportions of andesite lava clasts (2–6%) concentrated at the base of subunits or within planar laminae. No background hemipelagic sediment is preserved between the subunits, although this may have been eroded by the overlying flow.

[27] The 74–59 ka, 37–27 ka, and ~24 ka bioclastic deposits are only intersected in single cores; therefore, stratigraphic positioning is solely based on dating, and no observations of lateral change could be made.

5.4. Voluminous Mixed Bioclastic-volcaniclastic Deposit (~12–14 ka)

[28] A mixed bioclastic-volcaniclastic flow deposit was intersected in 20 cored locations within and adjacent to the Bouillante-Montserrat graben (Figures 3–5, and 6). The deposit comprises multiple subunits tens to hundreds of centimeters thick. An erosive base, grain size break, or an abrupt change in component abundance variation separates each subunit. Grain size within the subunits is predominantly within the sand range from -1.0ϕ (2 mm) to 4.5ϕ (0.045 mm). Individual subunits exhibit similar facies characteristics with normally graded tops and weakly reverse-graded

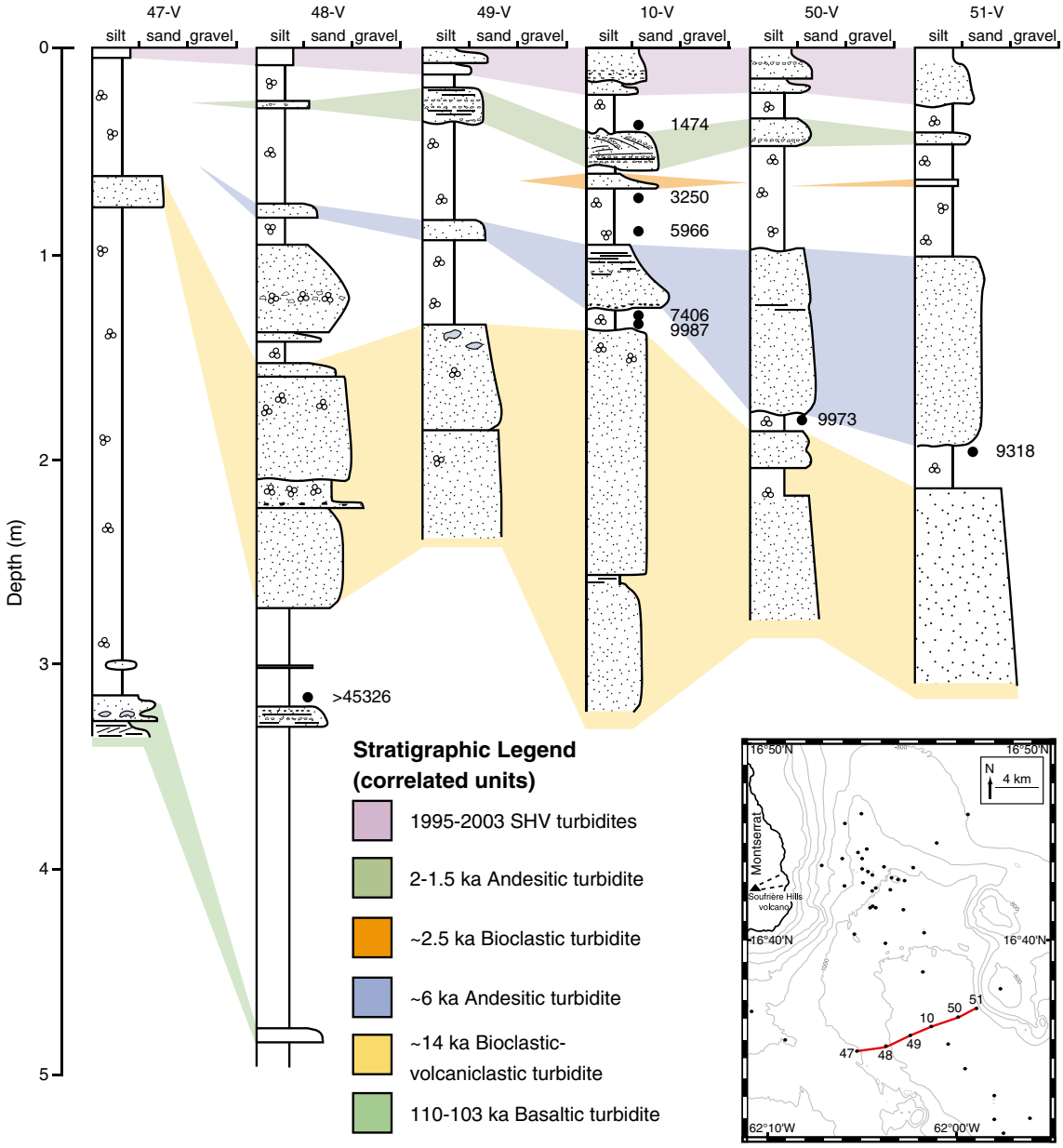

Figure 5. Correlated stratigraphic logs showing a transect through the central Bouillante-Montserrat graben, perpendicular to the longitudinal graben axis. Radiocarbon dates are provided in "years before present" with 2σ standard deviation; full details are in Table 1. Inset map shows the core numbers and locations.

bases. Individual horizons within the unit contain between 5% and 90% bioclastic grains and 10% and 95% volcaniclastic grains [*Trofimovs et al.*, 2010, their Figures 7, 9, and 10]. The bioclastic component tends to increase upwards within graded units, or towards the distal parts of the deposit [*Trofimovs et al.*, 2010], presumably due to slower settling of less dense bioclastic material. The integrated composition of the unit comprises subequal bioclastic and volcanic components. The bioclastic grains comprise benthonic and planktonic foraminifera, coral debris, shell fragments, and calcareous sand. The volcanic component includes angular to subrounded, variably altered andesitic lava fragments and broken plagioclase, hornblende, and orthopyroxene crystals. Reconstruction of the deposit volume provides a minimum estimate of 380×10^6 m^3 [*Trofimovs et al.*, 2010]. Stable isotope analysis together with complementary ^{14}C dates (Figure 2; Table 1) provide an age of ~12–14 ka.

[29] The deposit contains complex facies associations. North of the Bouillante-Montserrat graben, the deposit is represented as a single poorly sorted

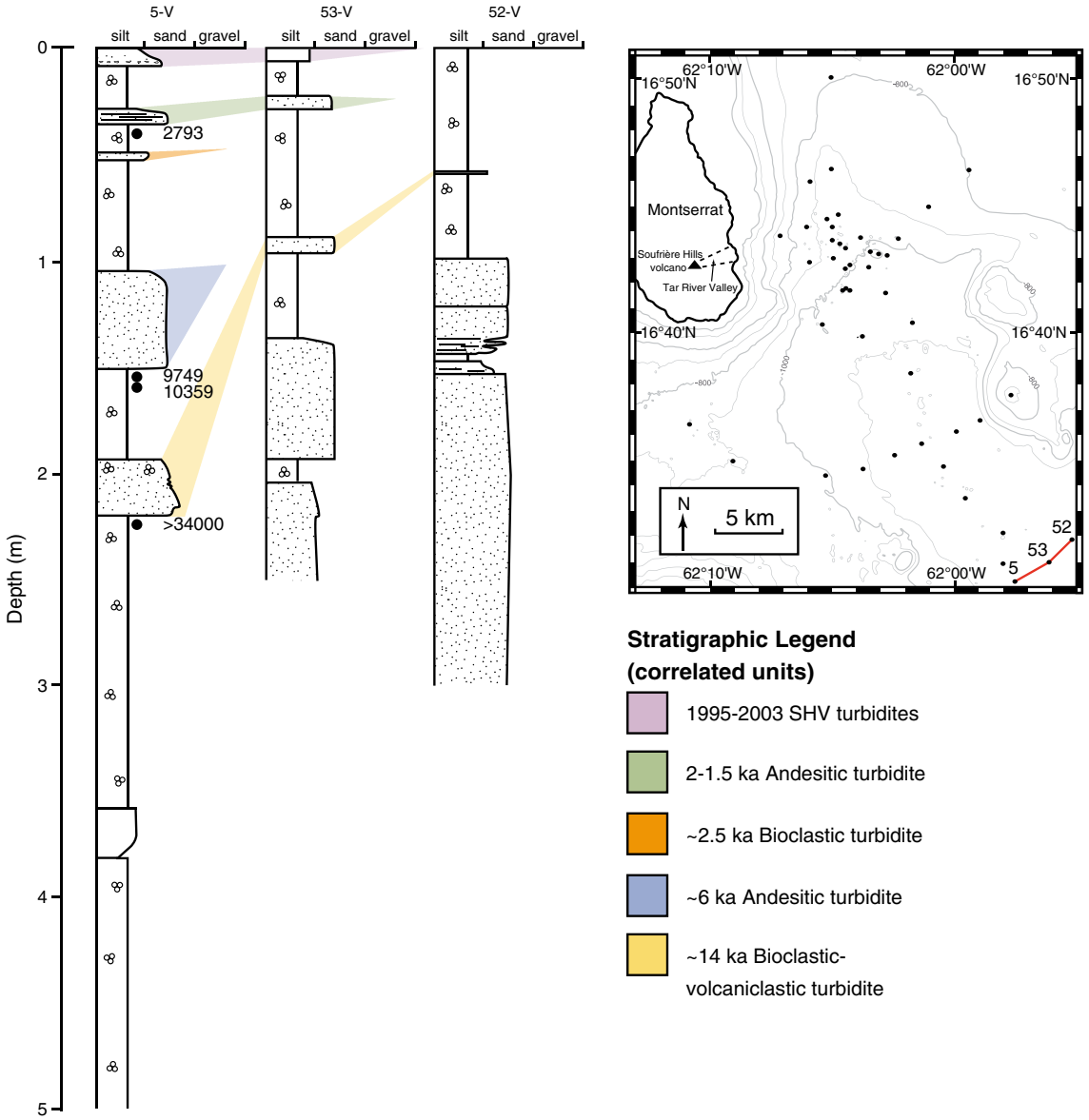

Figure 6. Correlated stratigraphic logs showing a transect through the southern Bouillante-Montserrat graben, perpendicular to the longitudinal graben axis. Radiocarbon dates are provided in "years before present" with 2σ standard deviation; full details are in Table 1. Inset map shows the core numbers and locations.

(1.08 to 1.38σ_ϕ), normally graded, fine to coarse sand (1.07 to 2.38 M_ϕ) depositional unit 60 cm in thickness. Radiocarbon dating directly above and below the depositional unit in core 35-V shows a large difference in age (Figure 2; *Trofimovs et al.* [2010]); ~14,000 years before present (B.P.) at the top of the flow and 38,000 years B.P. at the base. Using the average prebioclastic event sedimentation rate of 3.7 cm/kyr (from *Trofimovs et al.* [2010]) multiplied by the difference in age (24,000 years), approximately 88 cm of hemipelagic sediment has been removed by erosion at the base of the deposit.

[30] The mixed bioclastic-volcaniclastic deposit thickens markedly in the northern part of the Bouillante-Montserrat graben. Coring commonly did not intersect the base of the deposit (e.g., cores 12-V to 8-V, Figure 3), however, minimum thicknesses are consistently greater than 1 m. A single core (core 54-V, Figure 4) intersects a layer of poorly sorted, intensely altered and fractured andesitic lava fragments that appear to form the basal part of the mixed bioclastic-volcaniclastic deposit. Blocky, clasts of gray, yellow-green, and red altered lava rock are randomly distributed within a matrix of finer-grained altered lava fragments together with

crystals of magnetite, plagioclase, clinopyroxene, orthopyroxene, and pyrite. Vesicles are observed within the matrix adjacent to large hydrothermally altered clasts. The layer is massive with no evidence of grading or particle sorting. However, only a few centimeters of the deposit was recovered within the core and core catcher (the core catcher comprises a short tube with a set of teeth that prevent sediment from falling out of the base of the core barrel). AMS radiocarbon dating above the finer-grained top of the deposit in core 54-V (Figure 4; Table 1) indicates the deposit was emplaced slightly before 12730 ± 110 ka and therefore corresponds to the 12–14 ka mixed deposit.

[31] In the southern Bouillante-Montserrat graben, the mixed bioclastic-volcaniclastic deposit is represented as a single depositional unit (e.g., cores 7-V to 5-V, Figure 3) and is thinner (5–30 cm) and finer grained (0.0ϕ to 4.5ϕ; mean diameters $<3\phi$) compared with the northern graben. The deposit is characterized by a massive base overlain by millimeter-scale planar laminae and rare cross-stratification. The top of the deposits are normally graded and capped by mud or silt. The ~12–14 ka mixed bioclastic-volcaniclastic deposit is described in more detail by *Trofimovs et al.* [2010].

5.5. Volcanic-sourced Deposit (~6 ka)

[32] Stratigraphically overlying the ~12–14 ka mixed bioclastic-volcaniclastic flow deposit yet separated by hemipelagic sediment accumulation is a predominantly volcanic clast-rich deposit that preserves a single depositional unit confined within the Bouillante-Montserrat graben. Characteristically, the deposit thins and fines with distance from Montserrat and is represented by a reversely graded base and a normally graded top with millimeter- to centimeter-scale planar laminae observed throughout. The deposit comprises predominantly sand-sized particles (2.1 to 1.03 M_ϕ), with larger-granule sized particles observed towards the base of the most proximally cored deposits. It predominantly comprises andesite lava clasts and broken hornblende and plagioclase fragments (55–89%), with the remainder represented by biogenic particles including broken shell, coral, and benthonic and planktonic foraminifera. The proportion of biogenic fragments increases in the distal deposits, averaging 10–30% bioclasts proximally and 40–45% bioclasts distally.

[33] AMS radiocarbon dating and oxygen isotope profiles above the volcanic deposit provide an age estimate of around 6000 years B.P. (Figures 2 and 3), with individual ^{14}C dates above the deposit ranging from 5457 ± 177 to 6682 ± 218 (Table 1). Radiocarbon dates from beneath the volcanic deposit indicate age gaps between the top and base of the deposit, commonly around 2000 years, which is indicative of erosion of the underlying hemipelagic sediment to a depth of ~7 cm. This observation is supported by a scoured basal contact and the incorporated biogenic particles which may have been sourced from the carbonate shelf around Montserrat or incorporated from the underlying ~12–14 ka mixed bioclastic-volcaniclastic deposit.

5.6. Volcanic Ash-rich Horizons (~6.5–4.5 ka?)

[34] Two thin (3 cm), structureless deposits of volcanic ash, with planar top and basal contacts, are observed within core 54-V at depth intervals of 2.36–2.39 m and 2.43–2.46 m (Figure 4). Bioturbation appears to have caused minor mixing between the ash and adjacent hemipelagic sediment. AMS radiocarbon dates from above the upper horizon and below the lower horizon provide the ages of 6936 ± 217 years old and 6405 ± 191 years old, respectively (Table 1, Figure 4). These ages suggest that upper ash horizon is older than the lower and that both are older than the ~6 ka volcanic-sourced deposit (see above) that they stratigraphically overlie. Therefore, these dates are clearly unreliable. Although samples were chosen to avoid the effects of bioturbation where possible, the bioturbation observed within the ash horizons may have significantly vertically mixed the sampled foraminifera within the hemipelagic sediment. Without further radiocarbon analysis, the timing of deposition for these ash-rich horizons cannot be further refined. However, a 1 cm thick deposit of fine volcanic sand and ash is observed within cores 6-V, 7-V, and 40-V (Figures 3 and 4). AMS radiocarbon dating from core 6-V dates this deposit at between 4647 ± 221 years B.P. and 6187 ± 201 years B.P. (Table 1, Figure 3). These dates relate more accurately to the overall stratigraphic sequence and perhaps could correlate with one of the ash horizons observed in core 54-V and 40-V.

5.7. Bioclastic Deposit (~2.5 ka)

[35] A thin (2–8 cm) bioclastic deposit is observed in six cores within the southern Bouillante-Montserrat graben (cores 10-V to 5-V, Figure 3). The deposit is normally graded, massive, and contains fine to very fine-grained carbonate sand with a very small (2–5%) volcanic component. The volcanic component exhibits concentrated

abundances at the base of the deposit. AMS radiocarbon dates from the hemipelagic sediment above this stratigraphic unit indicate an age of approximately 2500 years B.P.

5.8. Volcanic-sourced Deposit (~2–1.5 ka)

[36] A voluminous volcaniclastic deposit has been identified at 2–1.5 ka by AMS radiocarbon dating and oxygen isotope profiles (Figures 2–5, and 6). It is cored in 31 localities and preserves a single depositional unit characterized by a scoured basal contact, a massive center and a normally graded top with common planar- and cross-laminae. Rip-up clasts of hemipelagic sediment are preserved at the top of the deposit in core 18-V, attesting to the erosive nature of the flow. The deposit is confined within the Bouillante-Montserrat graben and thins (from >172 cm to 8 cm) and fines (mean grain sizes from -1.27ϕ to $<3.0\phi$) with distance from Montserrat (Figures 3–5, and 6). The density and extent of core coverage for this unit allows a minimum deposit volume estimate of 103×10^6 m^3. This is a minimum volume as the base of the deposit was not intersected proximal to Montserrat, and the coring did not reach the most distal deposits within the southern Bouillante-Montserrat graben. Typically more than 95% of the clasts are volcaniclastic, comprising fresh and altered andesite lava fragments, hornblende, plagioclase, and magnetite crystals. An inherited biogenic component (2–5%) comprises shell and coral fragments, together with planktonic and benthonic foraminifera. The biogenic components are commonly concentrated within laminae in the thinner deposits, more distal to Montserrat.

5.9. Volcaniclastic Deposits from the Current Eruption of the Soufrière Hills Volcano (1995–2003)

[37] The uppermost stratigraphic units comprise a sequence of inverse and normally graded volcanic-sourced deposits that are the result of the current eruption of the Soufrière Hills volcano on Montserrat [*Trofimovs et al*., 2006; 2008]. A single vibrocore (core 23-V; Figure 3) penetrated a proximal pyroclastic ridge deposit from the dome collapse in July 2003. This core was positioned visually, using a rig-mounted video camera, between meter-scale volcanic blocks and therefore represents only the finer-grained matrix to these larger clasts. Core 23-V reveals a moderately to poorly sorted ($1.12–2.22\sigma_\phi$) angular breccia with grain sizes ranging from ~35 to 0.045 mm (-5ϕ to 4.5ϕ). The deposit is fines-poor containing <1 wt% silt sized particles (<0.063 mm) [*Trofimovs et al*., 2008]. Crude normal grading is preserved at the top of the deposit. The base was not intersected.

[38] Downstream from the thick, proximal pyroclastic ridges (>7 km), within the central and southern Bouillante-Montserrat graben, coring reveals a stacked series of volcaniclastic deposits (Figure 3). These deposits comprise predominantly sand and silt sized particles, with grain sizes ranging from 1.4 mm to <0.045 mm (-0.5ϕ to $<4.5\phi$). These deposits thin and fine from source, are moderately to well sorted and exhibit tractional structures such as planar- and cross-laminae. Scoured, inversely graded bases are common, together with normally graded, fine-grained tops. Soufrière Hills volcano-sourced andesitic lava fragments comprise the bulk of the deposit with subordinate broken, angular crystals, and an inherited bioclastic component (<3%). *Trofimovs et al*. [2006 and 2008] document these deposits in detail.

[39] Subsequent to the JR123 cruise in May 2005, there was another large-volume dome collapse down the Tar River Valley into the Bouillante-Montserrat graben (20 May 2006). The deposits from this recent collapse overlie and erode into the July 2003 submarine volcaniclastics and are described in *Trofimovs et al*. [2012].

6. Discussion

6.1. Fallout Deposits from Eruptions

[40] Only two volcaniclastic deposits, the ash horizons dated between 6.5 and 4 ka, can be attributed to emplacement mechanisms other than mass flow. However, there may be additional tephra layers present that are invisible to the naked eye (i.e., cryptotephras). The thin, planar, and structureless ash horizons are interpreted as ash fallout deposits, as opposed to thin turbidites, as they are monogenetic andesitic ash deposits with no evidence of tractional transport prior to deposition. In areas without bioturbation, the ash deposits do not contain an inherited bioclastic component eroded from underlying hemipelagic sediment, nor do they contain a large percentage of hydrothermally altered lava fragments, which may suggest collapse of older volcanic flank material into the ocean.

[41] Wind direction at Montserrat is on average towards the east at intermediate levels in the atmosphere (8–18 km; *Bonadonna et al*. [2002]). Assuming past Soufrière Hills volcano eruption behavior was similar to that observed in the current

eruption (lava dome collapse pyroclastic flows and Vulcanian explosions), we might expect more fall-out deposits preserved within the marine study area. Subsequent turbidity currents may have eroded such ash horizons. However, studies of the 1991 Pinatubo ash fall in the China Sea show that ash layers up to 3 to 4 cm thick can become completely bioturbated depending on the amount of subsequent biological activity [*Wetzel*, 2009].

[42] *Le Friant et al*. [2008] record high background levels of volcanic particles within hemipelagic sediment in a single core (CARMON 2) 55 km southwest of Montserrat. These authors searched for cryptotephras in this core and determined that normal hemipelagic accumulations may contain up to 16% glass shards, 28% poorly vesiculated volcanic particles, 20–60% crystals, and 20% lithics. This suggests that there is either a continuous large siliciclastic input from the volcanic islands of the Lesser Antilles into adjacent sedimentary basins, there has been thorough mixing of discrete volcanic horizons by biological activity to produce a more homogenized hemipelagic sediment pile, or both processes are occurring. This study focused on the visible tephra and turbidite deposits, so it is feasible that the record of explosive volcanic eruptions on Montserrat is preserved by cryptotephras that cannot be seen by visual examination of our cores [cf. *Le Friant et al*., 2008].

7. Mass Flow Deposits

[43] The marine stratigraphy within the Bouillante-Montserrat graben predominantly preserves mass flow deposits from volcanic, biogenic, or mixed sources, intercalated with hemipelagic sediment. Deposition from turbidity currents is indicated by the presence of well-developed grading, scoured deposit bases, and in some instances tractional structures, such as planar and cross-laminae [*Bouma*, 1962; *Kuenen*, 1966; *Allen* 1971; *Talling et al*., 2012].

7.1. Source of the 103–110 ka Basaltic Turbidite

[44] The oldest turbidite recognized in the graben cores is basaltic (~75%), with subordinate andesite (~25%). The deposit originates from the South Soufrière Hills volcanic center on Montserrat, which contains the only basaltic composition deposits on the island [*Rea*, 1974; *Smith et al*., 2007]. The subaerial South Soufrière Hills preserves both explosive scoria- and lapilli-pyroclastic fallout, flow and surge deposits, and lava flows [*Smith et al*., 2007]. *Harford et al*. [2002] date the subaerial South Soufrière Hills volcanism at circa 128–131 ka, suggesting that the South Soufrière Hills center built up during a relatively short period of time. *Le Friant et al*. [2008] observe primary basaltic scoria fallout dated in a marine sediment core west of Montserrat using oxygen isotope stratigraphy at circa 124–147 ka, which corresponds with the subaerial dates. The basaltic submarine turbidite was emplaced within the Bouillante-Montserrat graben between 103 and 110 ka. This suggests that the deposit resulted from collapse of pre-emplaced strata associated with the South Soufrière Hills complex, up to 30,000 years after the initial subaerial eruption.

[45] *Cassidy et al*. [2012] describe a potential laterally equivalent basaltic turbidite unit in submarine cores recovered to the west of the Bouillante-Montserrat graben. Predominantly basaltic turbidite (40% basaltic clasts and 35% broken crystals), with 25% andesitic clasts, lies between 1 and 3 m below the seafloor. [*Cassidy et al*. 2012] attribute the turbidite to a collapse of the South Soufriere Hills volcanic edifice, and shallow subsurface geophysical profiles provide evidence that this basaltic turbidite constitutes debris avalanche deposit 3 from *Le Friant et al*. [2004]. [*Cassidy et al*. 2012] have not dated this basaltic turbidite west of the Bouillante-Montserrat graben, but it is feasible that it is the lateral equivalent to the 103–110 ka event within the graben.

7.2. Source and Emplacement of Andesitic Turbidite (99–103 ka)

[46] This relatively thin (4 cm) turbidite is only encountered in a single core (Figure 3). It contains only a very small fraction of bioclastic material, which resembles that seen in the 1995 to recent turbidites at a similar distance from source. This suggests that than at least one andesitic dome-forming eruptive event may have occurred at ~100 ka, which broadly coincides with the *Harford et al*. [2002] extrusion date of 112 ka for Galways Dome.

7.3. Source and Emplacement of Bioclastic Turbidites (74–59 ka, 37–27 ka, ~24 ka and ~2.5 ka)

[47] These almost exclusively (> 95%) bioclastic turbidites most likely originated from submarine landslides off the shallow marine shelves around Montserrat or neighboring islands (Figure 1). Again, their timing coincides, within error, to dome-forming eruptions dated by *Harford et al*. [2002], indicating a possible connection between

the stability of the carbonate shelf around Montserrat during magma movement and eruptive events. Magma movement and volcanic activity are commonly cited as a potential cause of flank collapse on volcanic islands [e.g., *Moore et al*., 1989; *Masson et al*., 2002]. However, non-volcanic triggers such as earthquakes [Heezen and Ewing, 1952; *Gracia et al*., 2003], sea level fluctuation [*Quidelleur et al*., 2008], and sedimentation during glacial/interglacial cycles have also been linked to landslide initiation [*Kvalstad et al*., 2005]. Regardless of the original landslide trigger, an explosive eruption synchronous to turbidite deposition is unlikely in these cases due to the lack of significant pyroclastic components.

7.4. Source and Emplacement of Mixed Bioclastic-volcaniclastic Turbidite at ~12–14 ka

[48] The deposit emplaced at ~12–14 ka that contains broadly similar amounts of bioclastic and volcaniclastic grains is the thickest, coarsest, and most voluminous event emplaced in the study area during the last 110 ka. It also appears to have been one of the most powerful and erosive events. It is the only event to reach core site 35-V, where it has eroded ~88 cm of underlying sediment. It appears to have been equally erosive near core sites 5-V and 6-V at the distal end of the Bouillante-Montserrat graben, where sediment underlying the deposit is older than 34–39 ka.

[49] *Trofimovs et al*. [2010] concluded that the 12–14 ka event most likely originated from large nonvolcanic collapses of the carbonate shelf that surrounds either Antigua or Redonda. Volcanic material within the deposit was picked up as the flow moved past Montserrat according to this hypothesis. This hypothesis was based on the observation that the event had been highly erosive at core site 35-V, which is the site closest to Antigua and Redonda. However, the data presented here shows that this event was also very erosive at core sites 5-V and 6-V, which are furthest from Antigua and Redonda. This suggests that its source cannot be distinguished with confidence using basal erosion.

[50] Large coral fragments within the turbidites suggest a source at least partly within the photo-trophic zone. The presence of predominantly shallow water benthonic foraminifera species found in the ~12–14 ka bioclastic turbidite (e.g., *Peneroplis* spp. and *Amphistegina* spp.) support this. However, the composition of the bioclastic material cannot distinguish which island the flow originated from.

[51] The majority of the Lesser Antilles islands have well-developed carbonate platforms that could provide the source for carbonate material [*Adey and Burke*, 1979]. It is plausible that a carbonate platform has had time to develop around parts of Montserrat. Swath multibeam mapping of an embayment on the eastern side of Montserrat (potential "source area 3" of *Trofimovs et al*. [2010]; their Figure 2) has confirmed that there is no evidence of sea floor failure or landslide deposition in this vicinity. However, here we propose that the 12–14 ka event originated through a collapse involving both the volcanic edifice and a carbonate platform, which produced the large chute seen offshore from the Tar River Valley [cf. *Le Friant et al*., 2009]. This hypothesis is preferred because isopachs of the 12–14 ka deposit show that it is thickest offshore from the Tar River Valley, and it becomes finer grained with distance from this location and comprises relatively fine sand at core sites 35-V, 17-V, 5-V, and 6-V. This is supported by an interval of coarse-grained, altered andesitic clasts recovered at the base of core 54-V, which most likely records the top of the original debris avalanche that included parts of the volcanic edifice. This debris avalanche was deposited proximally, whereas the finer-grained mixed composition turbidite had a more extensive runout and deposited material radially from source. The 12–14 ka turbidite was the only mass flow from the Tar River Valley that deposited material to the north of the Bouillante-Montserrat graben (core 35-V), which potentially attests to its large volume and rapid emplacement dynamics. As such, we hypothesize it may be part of debris avalanche deposit 1 [cf. *Le Friant et al*., 2004; *Lebas et al*., 2011; *Watt et al*., 2012a; 2012b], involving the collapse of the Soufriere Hills volcano flanks and carbonate shelf. The previous hypothesis that it originates from Antigua or Redonda is less likely, as deep erosion at the base of the ~12–14 ka event occurs in the most distal core sites from those islands, and because the discovery of a proximal debris avalanche facies close to the base of the Tar River Valley corresponds to where the 12–14 ka deposit is thickest.

7.5. Source and Emplacement of the 1.5–2 ka and 6 ka Mixed Andesitic-rich Turbidites

[52] The andesitic volcaniclastic turbidites were sourced from the Soufrière Hills volcanic edifice as either primary pyroclastic flows into the ocean,

e.g., the deposits resulting from the current eruption of the Soufrière Hills volcano [cf. *Trofimovs et al*., 2006; 2008], or from volcanic sector collapse [cf. *Deplus et al*., 2001; *Le Friant et al*., 2004; *Boudon et al*., 2007; *Lebas et al*., 2011]. For example, the formation of English's Crater on the Soufrière Hills volcano was interpreted to have involved at least two collapses of the subaerial edifice at 3950 ± 70 years B.P. [*Roobol and Smith*, 1998] and 1990 ± 30 year B.P. [*Boudon et al*., 2007]. *Roobol and Smith* [1998] based the timing of the collapse on ^{14}C dating of charcoal from an andesite ash flow on the east of the island. We do not observe the submarine equivalent to this unit (Marker G; *Roobol and Smith* [1998]) in the marine cores. However, the submarine deposits from the second collapse (1990 ± 30 year B.P.; *Boudon et al*. [2007]) are preserved as a voluminous andesitic turbidite (2–1.5 ka) containing fresh and altered lava fragments, which compositionally corresponds to a collapse of the hydrothermally altered flanks of the Soufrière Hills volcano.

7.6. Origin and Timing of Deposit 1

[53] From the above discussion, there are two credible hypotheses for the origin of deposit 1 [*Deplus et al*., 2001; *Le Friant et al*., 2009; *Lebas et al*., 2011; Watt et al., 2012a]. The first hypothesis is that deposit 1 corresponds to events at ~6 ka and/or 2 ka that formed English's Crater on land and which emplaced turbidites within the Bouillante-Montserrat graben. The radiocarbon dates of *Boudon et al*. [2007] from terrestrial outcrops indicate that least one collapse occurred at ~2 ka. However, this may have been a minor later stage collapse that was not responsible for the large blocks in deposit 1. The second hypothesis is that the main collapse occurred at ~12–14 ka and formed the unit of stacked turbidites with a mixed bioclastic and volcaniclastic composition. Given that the ~12–14 ka event produced the thickest and coarsest deposit in the Bouillante-Montserrat graben, which was also the most powerful and erosive, this may be the most likely origin of deposit 1. However, further work is needed to determine its source and timing.

7.7. Frequency of Different Types of Mass Flows

[54] This study documents nine mass flow events during the last ~110 ka in addition to the 1995 to recent eruption deposits. Previous events that have generated similar mass flows to the 1995 to recent eruption are rare, suggesting that older episodes of volcanism may have differences in character. Events at 1.5–2 ka and 99–103 ka generated andesitic turbidites that reached the distal Bouillante-Montserrat graben and have a similar composition to those formed since 1995, but they comprise a single-graded unit rather than a series of stacked turbidites. A basaltic-rich turbidite at 103–100 ka most likely records a major flank collapse to the south of the island that involved failure of the basaltic South Soufriere Hills volcanic center [*Cassidy et al*., 2012]. Events involving a mixture of bioclastic and volcanic material occurred at ~12–14 ka and ~6 ka, and these most likely represent deep-seated failures of the volcanic edifice. The 12–14 ka event appears to have been particularly voluminous and powerful, and we now suggest its most likely origin to be from Montserrat [cf. *Trofimovs et al*., 2010]. Four almost exclusively bioclastic turbidites at 2.5 ka, 24 ka, 27–37 ka, and 59–74 ka appear to record failure of carbonate material from the flanks of Montserrat or nearby islands.

7.8. Emplacement Dynamics of Mass Flows and Their Consequences

[55] The mass flow deposits record a range of emplacement styles. The 1995 to recent dome collapses occurred every few years [e.g., *Cole et al*., 2002] and produced a series of stacked turbidite sands separated by turbidite mud [*Trofimovs et al*., 2006]. In contrast, the turbidites deposited at 6 ka and 1.5–2 ka are characterized by a single depositional unit with a reversely graded base and normally graded bulk which preserves a variety of tractional sedimentary structures such as planar and cross-laminae. This suggests that the source collapse occurred as a single failure and produced a turbidity current that waxed and waned. The 12–14 ka event has a highly complex stacking pattern that suggests it was emplaced in a series of stages. The remaining events are only seen in distal cores, where they comprise a single-graded sequence. It is uncertain whether they represent single events or events with multiple stages where the other stages generated only short runout turbidity currents.

[56] Mass flows into the ocean will displace water, which can form a tsunami [*Latter*, 1981; *McGuire*, 2006]. The collapse dynamics of a landslide into the ocean, such as volume, velocity, and water depth, are important for interpreting the scale of the tsunami hazard [*Harbitz*, 1992; *Harbitz et al*., 2006; *Masson et al*., 2006]. The single-failure

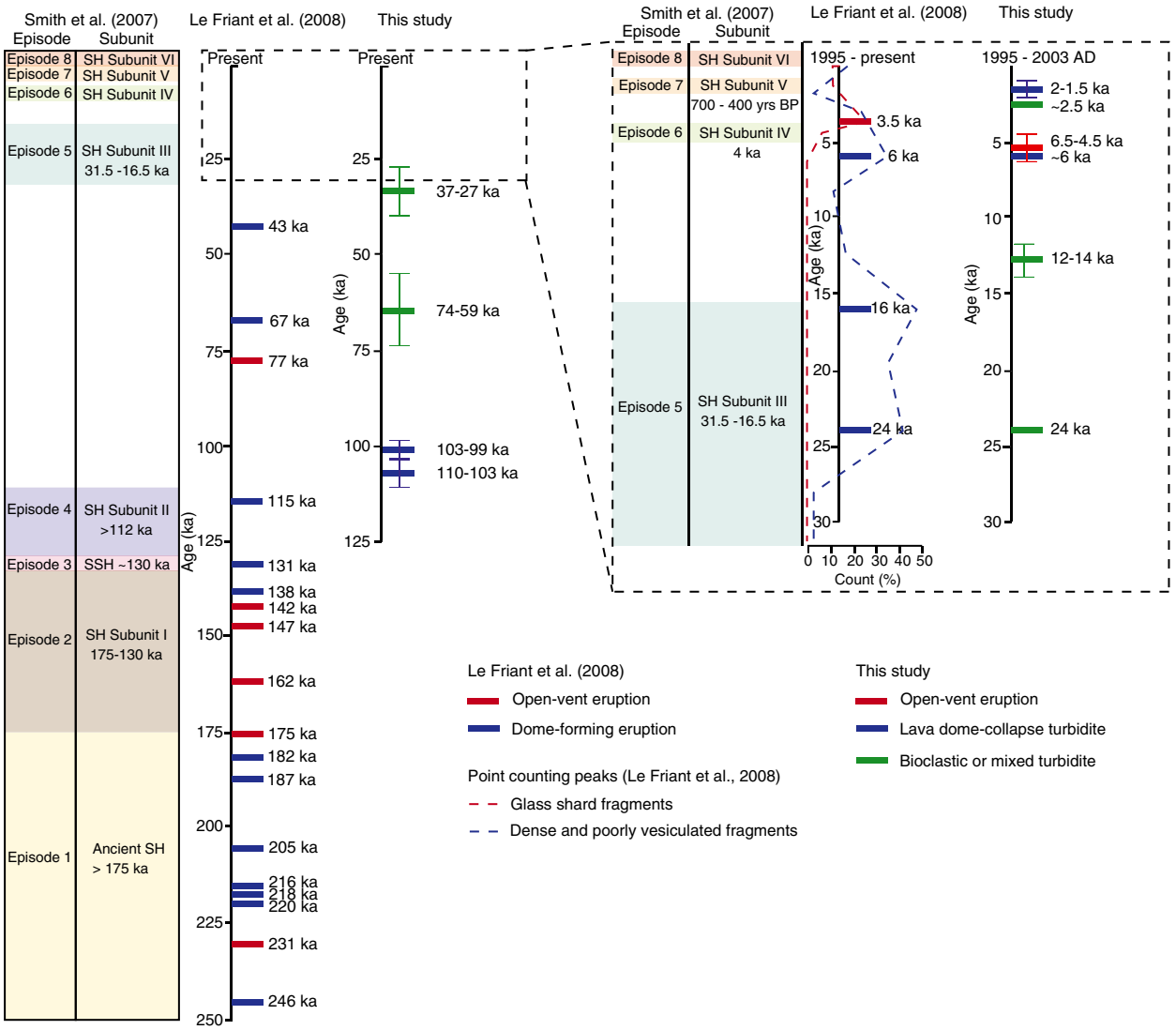

Figure 7. Diagram comparing the dated subaerial stratigraphic sequence for the Soufrière Hills and south Soufrière Hills volcanic complex [*Smith et al.*, 2007], with a marine core southwest of Montserrat [*Le Friant et al.*, 2008] and findings from this study.

events, wherein the entire collapse volume enters the ocean in one go, are hypothesized to produce larger waves than an incremental collapse involving smaller volume failures over a longer amount of time [*Wynn and Masson*, 2003; *Hunt et al.*, 2011]. It is therefore apparent from the Bouillante-Montserrat graben submarine record, which contains small and moderate volume mass flows and evidence of both single- and multiple-failure emplacement, that Montserrat poses a significant and varied tsunami risk.

[57] The 1995–2003 dome collapses into the ocean have produced tsunamis that have run up 5–15 m on the Montserratian coast and reached neighboring islands 80 km away [*Herd et al.*, 2005]. These dome collapses were incremental in character [*Cole et al.*, 2002; *Herd et al.*, 2005; *Trofimovs et al.*, 2008]. In comparison, the thicker turbidite deposits at 6 ka and 1.5–2 ka (and possibly the older bioclastic and volcaniclastic turbidites), which record evidence of single-failure collapse dynamics, indicate even greater tsunami amplitude potential than that observed during the current eruption.

[58] Submarine slope failures and volcanic flank collapse have produced some of the largest mass flows on Earth (e.g., the Canary Islands; *Masson et al.* [2002; 2006], and the Hawaiian islands; *Moore et al.* [1989]) and have been linked to potentially catastrophic tsunamis [e.g., *Ward and Day*, 2001]. *Boudon et al.* [2007] show that large-volume landslides are also a common occurrence within the

Lesser Antilles island arc, with several deposits identified around Montserrat [*Deplus et al*., 2001; *Le Friant et al*., 2004; *Lebas et al*., 2011; *Watt et al*., 2012b]. The 12–14 ka mixed turbidite preserves characteristics analogous to such a volcanic edifice and shallow marine shelf collapse, and we link it to deposit 1 of the previous studies. The stacked turbidites of the 12–14 ka deposit are indicative of incremental collapse of the estimated minimum volume of 380×10^6 m^3, which would significantly lessen its tsunamigenic potential. Therefore, although the volume of the collapse exceeds the single-failure events, its piecemeal collapse dynamic may have subdued the maximum amplitude of resulting tsunamis.

7.9. Comparison between the Timing of Mass Flows and Volcanic Eruptions

[59] Figure 7 compares the Bouillante-Montserrat graben marine stratigraphy with the Soufrière Hills volcano subaerial stratigraphy [*Roobol and Smith*, 1998; *Harford et al*., 2002; *Smith et al*., 2007] and the marine stratigraphy observed in a single core 55 km southwest of Montserrat [*Le Friant et al*., 2008].

[60] *Le Friant et al*. [2008] identify peaks in dense volcanic clast (dome-forming eruptions) and volcanic glass shard (open-vent eruptions) abundances within hemipelagic sediment and attribute these peaks to deposits from dome collapse or explosive eruptions, respectively. In total, *Le Friant et al*. [2008] recognize at least 15 eruptive periods from the Soufrière Hills and South Soufrière Hills volcano within the marine volcaniclastic deposits. Figure 7 depicts the 12 events recognized by *Le Friant et al*. [2008] with ages less than 150 ka. Only four events are recognized by Le Friant as being from open-vent, explosive eruptions, whereas the remainder are sourced from dome-forming eruptions, which may have collapsed into the ocean many thousands of years later. It is therefore clear from our study and that of *Le Friant et al*. [2008] that volcaniclastic turbidites are better preserved than visible fallout deposits in cores from the Bouillante-Montserrat graben and surrounds.

[61] The marine sediment record predominantly preserves evidence of volcanic edifice or dome collapses, while the subaerial record additionally includes less powerful and shorter runout events, making it difficult to directly compare the subaerial and submarine stratigraphies. For example, *Harford et al*. [2002] provide an ^{39}Ar/^{40}Ar date for the construction of Perches Dome in the Soufrière Hills volcanic complex at 24.1 ka. *Le Friant et al*. [2008] record a submarine flow event at this age: however, without further geochemical fingerprinting of the submarine flow to Perches Dome, it remains inconclusive as to the connection between the two deposits. This study records a bioclastic turbidite at circa 24 ka, which is not interpreted to be related to a constructional event with the Soufrière Hills volcano history. Similarly, the collapse event at 12–14 ka that formed the mixed bioclastic-volcaniclastic unit is not associated with a major eruption in either the terrestrial or *Le Friant et al*. [2008] record.

[62] The record of eruption from the basaltic South Soufrière Hills is preserved in all of the studies summarized by Figure 7. The *Le Friant et al*. [2008] marine record supports the subaerial dates that suggest the basaltic complex erupted circa 130 ka. This suggests that the Carmon 2 core in the *Le Friant et al*. [2008] study preserves primary pyroclastic deposits, emplaced during the original eruption at circa 130 ka. Therefore, fallout from the South Soufrière Hills eruptions was to the southwest of Montserrat. We do not observed such deposits southeast of Montserrat within the Bouillante-Montserrat graben. Instead, the cores preserve a record of basaltic-rich mass wasting of the South Soufrière Hills volcanic complex that occurred 20–30 thousand years after the initial basaltic eruptions.

[63] Our results highlight that the threat from landslides and tsunamis around Montserrat and other volcanic islands is not confined to periods of volcanic activity. The Bouillante-Montserrat graben record shows that tsunamigenic volcano flank and carbonate shelf collapse occurs in the absence of eruptions and that other factors, such as seismic activity, sea level fluctuation, and climate-induced sediment loading on submarine shelves should also be considered.

8. Conclusions

[64] This study analyzes arguably the most comprehensive sediment core data set offshore from a volcanic island. These cores illustrate how volcanic island growth and collapse over a period of 110 ka involved voluminous and extensive mass flows with highly variable composition. In addition, submarine mass flows generated by a series of volcanic dome collapses during the 1995 to recent eruption of the Soufriere Hills volcano are also preserved. Four of the mass flows comprise almost exclusively bioclastic particles and occurred

at 74–59 ka, 27–37 ka, 24 ka, and 2.5 ka. These non-volcanic deposits most likely resulted from collapse of carbonate shelves around Montserrat or adjacent islands. The other volcanic mass flow deposits differ from those generated during the current eruption. This suggests that previous eruptions may have differed from the repeated dome collapses seen since 1995, which caused pyroclastic flows to enter the ocean. The oldest mass flow deposit seen in these cores is a turbidite rich in basaltic grains that most likely originated through collapse of the basaltic South Soufriere Hills center at 103–110 ka, some 20–30 ka after basaltic eruptions formed this center.

[65] A ~1.8 km^3 blocky debris avalanche deposit (deposit 1) that extends from a chute in the shelf records a particularly deep-seated failure of the volcanic edifice. Deposit 1 was most likely formed by a collapse event on Montserrat at ~12–14 ka that included almost equal amounts of the volcanic edifice and a coeval carbonate shelf, which emplaced a mixed bioclastic-volcaniclastic turbidite in a complex series of stages. This origin is most likely because the ~12–14 ka deposit is the largest volume, coarsest grained, and most erosive event recorded in the cores, and the deposit thickens and coarsens towards the Soufriere Hills Volcano. The ~12–14 ka event does not appear to be associated with major eruptions of the volcano, as recorded in the information available from terrestrial sequences or distal tephra layers in marine cores [*Harford et al*., 2002; *Le Friant et al*., 2008].

[66] The collective study on and offshore of Montserrat highlights the difficulties in reconstructing accurate eruption histories for island volcanoes. Considering the wealth of data obtained, it remains difficult to determine if the lack of visible pyroclastic airfall deposits is a primary effect of volcano activity or preservation biases in the marine realm. We can conclude that turbidites are well preserved in the marine record and provide a good record of collapse dynamics, such as waxing and waning energy levels and single or multiple failure; however, we caution that they do not necessarily represent primary volcanic activity. Consequently, natural hazards associated with volcanic arcs are not confined to volcanic eruption, as the construction of an island volcano is equally influenced by destructive mass flow processes.

Acknowledgments

[67] This work was supported by the NERC grant NER/A/S/2002/00963. Radiocarbon dating and stable isotope analysis was supported by NERC (grants RCL/1164.0306, RCL/1229.0407 and IP/992/1107, respectively). The authors would like to thank the British Geological Survey for their technical support and expertise and the captain, crew, and scientific team on the RRS *James Clark Ross* for their invaluable assistance. R.S.J.S. acknowledges a European Research Council Advanced Grant (Project VOLDIES). Two anonymous reviewers are thanked for their helpful comments.

References

Adey, W. H., and R.,Burke (1979), Holocene bioherms (algal ridges and bank-barrier reefs) of the eastern Caribbean, *Geol. Soc. Am. Bull.*, *87*, 95–109.

Allen, J. R. L. (1971), Instantaneous sediment deposition rates deduced from climbing-ripple cross-lamination, *J. Geol. Soc. London*, *127*, 553–561.

Bonadonna, C., et al. (2002), Tephra fallout in the eruption of Soufriere Hills Volcano, Montserrat, in The Eruption of Soufriere Hills Volcano, Montserrat, from 1995 to 1999, edited by Druitt, T. H., Kokelaar, B. P., *21*, 483–516, Geological Society of London, Memoirs.

Boudon, G., A., Le Friant, J.-C., Komorowski, C., Deplus, and M. P. Semet (2007), Volcano flank instability in the Lesser Antilles Arc: Diversity of scale, processes, and temporal recurrence, *J. Geophys. Res.*, *112*, B08205, doi:10.1029/2006JB004674.

Bouma, A. H. (1962), *Sedimentology of Some Flysch Deposits: A Graphic Approach to Facies Interpretation*, p. 168, Elsevier, Amsterdam.

Bouysse, P., D., Westercamp, and P. Andreieff (1990), The Lesser Antilles Island Arc, in *Proceedings of the Ocean Drilling Program, Scientific Results*, edited by Moore, J. C., A., Mascle, *110*, 29–44, Ocean Drilling Program, College Station, TX.

Briden, J. C., D. C., Rex, A. M., Faller, and J. F. Tomblin (1979), K-Ar geochronology and paleomagnetism of volcanic rocks in the Lesser Antilles island arc, *Phil. Trans. R. Soc. London*, *291*, 485–528.

Cassidy, M., J., Trofimovs, S. F. L., Watt, M. R., Palmer, R. N., Taylor, T. M., Gernon, P. J., Talling, and A. Le Friant (2012), Multi-stage collapse events in the South Soufriere Hills, Montserrat, as recorded in marine sediment cores, *J. Geol. Soc. London*, in press.

Cole, P. D., E. S., Calder, R. S. J., Sparks, A. B., Clarke, T. H., Druitt, S. R., Young, R. A., Herd, C. L., Harford, and G. E. Norton (2002), Deposits from dome-collapse and fountain-collapse pyroclastic flows at Soufriere Hills Volcano, Montserrat, in The Eruption of Soufriere Hills Volcano, Montserrat, from 1995 to 1999, edited by Druitt, T. H., B. P., Kokelaar, 2002, v. *21*, p. 231–262, Geological Society of London, Memoirs.

Deplus, C., A., Le Friant, G., Boudon, J.-C., Komorowski, B., Villemant, C., Harford, J., Ségoufin, and J.-L. Cheminée (2001), Submarine evidence for large-scale debris avalanches in the Lesser Antilles Arc, *Earth Planet. Sci. Lett.*, *192*, 145–157, doi:10.1016/S0012-821X(01)00444-7.

Druitt, T. H., and B. P. Kokelaar (eds) (2002), The Eruption of Soufrière Hills Volcano, from 1995 to 1999, *21*, 645 pp, Geological Society, London, Memoirs.

Freeman, S. P. H., A., Dougans, L., McHargue, K. M., Wilcken, and S., Xu (2008), Performance of the new single stage accelerator mass spectrometer at the SUERC, *Nuclear*

Instruments and Methods in Physics Research, B, *266*, 2225–2228.

Gracia, E., J., Danobeitia, J., Verges, and Team P. A. R. S. I. F. A. L. (2003), Mapping active faults offshore Portugal (36 N–38 N): Implications for seismic hazard assessment along the southwest Iberian margin, *Geology*, *31*, 83–86, doi:10.1130/0091-7613(2003)031<0083:MAFOPN>2.0.CO;2.

Grindlay, N. R., M., Hearne, and P. Mann (2005), High risk of tsunami in the Northern Caribbean, *Eos Trans. Amer. Geophys. Union*, *86*(12), 121–132, doi:10.1029/2005EO120001.

Harbitz, C. B. (1992), Model simulations of tsunamis generated by the Storegga Slides, *Mar. Geol.*, *105*, 1–21, doi:10.1016/0025-3227(92)90178-K.

Harbitz, C. B., F., Lovholt, G., Pedersen, and D. G. Masson (2006), Mechanisms of tsunami generation by submarine landslides: A short review, *Norw. J. Geol.*, *86*, 255–264.

Harford, C. L., M. S., Pringle, R. S. J., Sparks, and S. R. Young (2002), The volcanic evolution of Montserrat using $^{40}Ar/^{39}Ar$ geochronology, in The Eruption of Soufriere Hills Volcano, Montserrat, from 1995 to 1999, edited by Druitt, T. H., Kokelaar, B. P. 2002, v. *21*, p. 93–113, Geological Society of London, Memoirs.

Heezen, B. C. and M., Ewing (1952), Turbidity currents and submarine slumps, and the 1929 Grand Banks Earthquake, *Am. J. Sci.*, *250*, 775–793.

Herd, R. A., M., Edmonds, and V. Bass (2005), Catastrophic lava dome failure at Soufrière Hills Volcano, Montserrat 12–13 July 2003, *J. Volcanol. Geotherm. Res.*, *148*(3–4), 234–252, doi:10.1016/j.jvolgeores.2005.05.003.

Hunt, J. E., R. B., Wynn, D. G., Masson, P. J., Talling, and D. A. H. Teagle (2011), Sedimentological and geochemical evidence for multistage failure of volcanic island landslides: A case study from Icod landslide on north Tenerife, Canary Islands, *Geochem. Geophys. Geosyst.*, *12*, Q12007, doi:10.1029/2011GC003740.

Kuenen, P. H. (1966), Matrix of turbidites: experimental approach, *Sedimentology*, *7*, 267–297.

Kvalstad, T. J., L., Andresen, C. F., Forsberg, K., Berg, P., Bryn, and M., Wangen (2005), The Storegga slide: Evaluation of triggering sources and slide mechanics, *Mar. Petrol. Geol.*, *22*, 245–256, doi:10.1016/j.marpetgeo.2004.10.019.

Latter, J. H. (1981), Tsunamis of volcanic origin: Summary of causes, with particular reference to Krakatoa, 1883, *Bull. Volcanol.*, *44* (3), 467–490.

LeBas, E., A., Le Friant, G., Boudon, S. F. L., Watt, P. J., Talling, N., Feuillet, C., Deplus, C., Berndt, and M. E. Vardy (2011), Multiple widespread landslides during the long-term evolution of a volcanic island: Insights from high-resolution seismic data, Montserrat, Lesser Antilles, *Geochem. Geophys. Geosyst.*, *12*, Q05006, doi:10.1029/2010GC003451.

Le Friant, A., C. L., Harford, C., Deplus, G., Boudon, R. S. J., Sparks, R. A., Herd, and J. C. Komorowski (2004), Geomorphological evolution of Montserrat (West Indies): Importance of flank collapse and erosional processes, *J. Geol. Soc. London*, *161*, 147–160, doi:10.1144/0016-764903-017.

Le Friant, A., E. J., Lock, M. B., Hart, G., Boudon, R. S. J., Sparks, M. J., Leng, C. W., Smart, J.-C., Komorowski, C., Deplus, and J. K. Fisher (2008), Late Pleistocene tephrochronology of marine sediments adjacent to Montserrat, Lesser Antilles volcanic arc, *J. Geol. Soc. London*, *165*, 279–289, doi:10.1144/0016-76492007-019.

Le Friant, A., C., Deplus, G., Boudon, R. S. J., Sparks, J., Trofimovs, and P. J. Talling (2009), Submarine deposition of volcaniclastic material from the 1995–2005 eruptions of Soufriere Hills volcano, Montserrat, *J. Geol. Soc.*, *166*, 171–182, doi:10.1144/0016-76492008-047.

Le Friant, A., C., Deplus, G., Boudon, N., Feuillet, J., Trofimovs, J.-C., Komorowski, R. S. J., Sparks, P., Talling, S., Loughlin, and G. Ryan (2010), Eruption of Soufrière Hills (1995–2009) from an offshore perspective: Insights from repeated swath bathymetry surveys, *Geophys. Res. Lett.*, *37*, L11307, doi:10.1029/2010GL043580.

Martinson, D. G., N. G., Pisias, J. D., Hays, J., Imbrie, T. C., Moore, and N. Shackleton (1987), Age dating and the orbital theory of the ice ages: Development of a high-resolution 0 to 300,000-year chronostratigraphy, *Quaternary Res.*, *27*, 1–30.

Masson, D. G., A. B., Watts, M. R. J., Gee, R., Irgeles, N. C., Mitchell, T. P., Le Bas, and M. Canals, (2002), Slope failures on the flanks of the western Canary Islands, *Earth Sci. Rev.*, *57*, 1–35, doi:10.1016/S0012-8252(01)00069-1.

Masson, D. G., C. B., Harbitz, R. B., Wynn, G., Pedersen, and F. Lovholt (2006), Submarine landslides: Processes, triggers and hazard prediction, *Phil. Trans. Roy. Soc. Am.*, *364*, 2009–2039.

McGuire, W. J. (2006), Lateral collapse and tsunamigenic potential or marine volcanoes, in Mechanisms of Activity and Unrest at Large Calderas, edited by C. Troise, and D. De Natale, *269*, 121–140, Geol. Soc. Spec. Publ..

Moore, J. G., D. A., Clague, R. T., Holocomp, P. W., Lipman, W. R., Normark, and M. E. Torresan (1989), Prodigious submarine landslides on the Hawaiian Ridge, *J. Geophys. Res.*, *94*, 17465–17484.

Nagle, F., J. J., Stipp, and D. E. Fisher, (1976), K-Ar geochronology of the Limestone Caribbees and Martinique, Lesser Antilles, West Indies, *Earth Planet. Sci. Lett.*, *29*, 401–412.

Quidelleur, X., A., Hildenbrand, and A. Samper (2008), Casual link between Quaternary paleoclimatic changes and volcanic island evolution, *Geophys. Res. Lett.*, *35*, L02303, doi:10.1029/2007GL031849.

Rea, W. J., (1974), The volcanic geology and petrology of Montserrat, West Indies, *J. Geol. Soc. London*, *130*, 341–366.

Roobol, M. J., and A. L., Smith (1998), Pyroclastic stratigraphy of the Soufrière Hills volcano, Montserrat: implications for the present eruption, *Geophys. Res. Lett.*, *25*, 3393–3396.

Slota, P. J., A. J. T., Jull, T. W., Linick, and L. J. Toolin (1987), Preparation of small samples for C-14 accelerator targets by catalytic reduction of CO, *Radiocarbon*, *29*, 303–306.

Smith, A. L., M. J., Roobol, J. H., Schellekens, and G. S. Mattioli (2007) Prehistoric stratigraphy of the Soufrière Hills-South Soufrière Hills volcanic complex, Montserrat, West Indies, *The Journal of Geology*, *115*, 115–127, doi:10.1086/509271.

Talling, P. J., E. J., Sumner, D. G., Masson, and G. Malgesini (2012), Subaqueous sediment density flows: Depositional processes and deposit types, *Sedimentology*, *59* (7), 1937–2003, doi:10.1111/j.1365-3091.2012.01353.x.

Trofimovs, J., et al. (2006), Submarine pyroclastic deposits formed at the Soufrière Hills Volcano, Montserrat (1995–2003): What happens when pyroclastic flows enter the ocean? *Geology*, *34* (7), 549–552, doi:10.1130/G22424.1.

Trofimovs, J., R. S. J., Sparks, and P., Talling (2008). Anatomy of a submarine pyroclastic flow and associated turbidity current: July 2003 dome collapse, Soufrière Hills volcano, Montserrat, West Indies, *Sedimentology*, *55*, 617–634, doi:10.1111/j.1365-3091.2007.00914.x.

Trofimovs, J., et al. (2010), Evidence for carbonate platform failure during rapid sea level rise; ca 14,000 year old bioclastic flow deposits in the Lesser Antilles, *Sedimentology*, *57*, 735–759, doi:10.1111/j.1365-3091.2009.01117.x.

Trofimovs, J., et al. (2012), Submarine pyroclastic deposits formed during the 20th May 2006 dome collapse of the Soufriere hills volcano, Montserrat, *Bull. Volcanol.*, *74*(2), 391–405, doi:10.1007/s00445-011-0533-5.

Voight, B., et al. (2002), The 26 December (Boxing Day) 1997 sector collapse and debris avalanche at Soufrière Hills Volcano, Montserrat, in *The Eruption of Soufrière Hills Volcano, Montserrat, from 1995 to 1999*, edited by Druitt, T. H., and B. P. Kokelaar, *21*, 363–407, Geological Society, London, Memoirs.

Voight, B., et al. (2006), Unprecedented pressure increase in deep magma reservoir triggered by lava-dome collapse, *Geophys. Res. Lett.*, *33*, L03312, doi:10.1029/2005GL024870.

Wadge, G. (1984), Comparison of volcanic production rates and subduction rates in the Lesser Antilles and Central America, *Geology*, *12*, 555–558, doi:10.1130/0091-7613(1984)12>555:COVPRA>2.0.CO;2.

Ward, S. N., and S. J. Day (2001). Cumbre Vieja volcano - potential collapse and tsunami at La Palma, Canary Islands, *Geophys. Res. Lett.*, *28*, 3397–3400, doi:10.1029/2001GL013110.

Watt, S. F. L., et al. (2012a), Combinations of volcanic-flank and seafloor-sediment failure offshore Montserrat, and their implications for tsunami generation, *Earth Planet. Sci. Lett.*, *319*, 228–240, doi:10.1016/j.epsl.2011.11.032.

Watt, S. F. L., et al. (2012b), Widespread and progressive seafloor-sediment failure following volcanic debris avalanche emplacement: landslide dynamics and timing offshore Montserrat, Lesser Antilles, *Marine Geology*, *323–325*, 69–94, doi:10.1016/j.margeo.2012.08.002.

Wetzel, A., (2009), The preservation potential of ash layers in the deep-sea: The example of the 1991-Pinatubo ash in the South China Sea, *Sedimentology*, *56*, 1992–2009, doi:10.1111/j.1365-3091.2009.01066.x.

Wynn, R. B., Masson, D. G., (2003). Canary island landslides and tsunami generation: Can we use turbidite deposits to interpret landslide processes. In: Locat, J., Mienert, J. (eds), *Submarine Mass Movements and Their Consequences:* 1st International Symposium, Adv. Nat. and Technol. Hazard Res., 19, 325–332.

Xu, S., R. Anderson, C. Bryant, G. T. Cook, A. Dougans, S. Freeman, P. Naysmith, C. Schnabel, and E. M. Scott (2004), Capabilities of the new SUERC 5MV AMS facility for 14C dating. *Radiocarbon, 46*, 59–64.

Young, S. R., Voight, B., Barclay, J., Herd, R. A., Komorowski, J.-C.., Miller, A. D., Sparks, R. S. J., Stewart, R. C., (2002), Hazard implications of small-scale ediface instability and sector collapse: A case history from Soufrière Hills Volcano, Montserrat, in *The Eruption of Soufrière Hills Volcano, Montserrat, from 1995 to 1999*, Druitt, T. H., and B. P. Kokelaar, *21*, 349–361, Memoirs, Geological Society, London.

Zellmer, G., C. J., Hawkesworth, and R. S. J. Sparks 2003, Geochemical evolution of the Soufrière Hills Volcano, Montserrat, Lesser Antilles Volcanic Arc, *J. Petrol.*, *44*, 1349–1374, doi:10.1093/petrology/44.8.1349.